THE PREVALENCE OF KIT D816V IN MYELOPROLIFERATIVE NEOPLASMS AND IMPACT ON DISEASE SEVERITY

Author: Erik Moedt (S2899280)

Supervisors: dr. André Mulder & Abdulrazzaq Alheraky

Rijksuniversiteit Groningen, 30-05-2021

Abstract

MPN is characterized by overproduction of a diversity of blood cells, BCR-ABL-1 negative MPNs commonly comprise PV, ET and PMF. These subtypes are generally characterized by JAK2 V617F, CALR or MPL driver mutations. In SM, accumulation of mast cells in bone marrow or other visceral organs occurs and the KITD816V mutation is virtually inseparable from SM. In about 30% of SM cases, an associated hematologic neoplasm of non-mast cell lineage is present simultaneously. The AHN component is predominantly represented by MPNs.

In this study, prevalence of KIT D816V in MPNs and clinical implications of said co-occurrence were investigated. Whereas previous research on this matter generally utilized either NGS or qPCR, a more sensitive assay using ddPCR was carried out here. Further investigation on clinical implications was done with diagnostic scoring and available NGS data. In total, 320 MPN patients were included in the KIT D816V assay, of which 29 proved to be positive (9,1%). This finding exceeds previous studies, wherein a prevalence of 5,8% was found. Out of 369 samples, 50 remained inconclusive after re-testing, due to single-positivity or technical inadequacy. Therefore, actual prevalence might be slightly higher than found here. Additionally, KIT-positive patients showed an inclination towards JAK2 V617F (93,1%), as compared to the total cohort (79,4%).

Diagnostic scoring showed a higher frequency of deteriorated diagnoses such as MDS, AML, SM-MPN or severe MF progression (MF>2) in KIT-positive cases (55,6%), in contrast to KIT-negative cases (39,9%). This finding is underlined by analysis of NGS data, in which KIT-positive patients (80%) were classified with a deteriorated diagnose significantly more often than KIT-negative cases (45,7%). Cohort size (n = 75) was limited however, rendering these results statistically unsubstantial. An attempt was made to investigate correlation of additional passenger mutations in KIT-positive and KIT-negative patients within the NGS cohort. Although likewise hindered by cohort size, a predominant inclination towards less common mutations such as KRAS, PTNP11 and GATA2 was seen only in KIT-positive patients.

The co-occurrence of KIT D816V in MPN might hold more clinical implications than previously thought, as witnessed within this study. Furthermore, prevalence of KIT within MPN exceeded preceding research significantly, illustrating the necessity of further research and clinical consideration.

List of Abbreviations

advSM	Advanced Systemic Mastocytosis
ASM	Aggressive Systemic Mastocytosis
B-findings	Burden of disease findings
BM	Bone Marrow
BMM	Bone Marrow Mastocytosis
CALR	Calreticuline
CEL-NOS	Chronic Eosinophilic Leukemia, not otherwise specified
C-findings	Cytoreduction-requiring findings
CHIP	Clonal Hematopoiesis of Intermediate Potential
CM	Cutaneous Mastocytosis
CML	Chronic Myeloid Leukemia
CMML	Chronic MyeloMonocytic Leukaemia
CNL	Chronic Neutrophilic Leukemia
ddPCR	droplet digital Polymerase Chain Reaction
ET	Essential Thrombocythemia
GI	GastroIntestinal
Hb	Hemoglobin
HSC	Hematopoietic Stem Cell
Ht	Hematocrit
ISM	Indolent Systemic Mastocytosis
JAK	Janus kinase
MCAS	Mast Cell Activation Syndrome
MCL	Mast Cell Leukemia
MCS	Mast Cell Sarcoma
MPL	Myeloproliferative leukemia protein
MPN	MyeloProliferative Neoplasm
MPN-U	MPN, Unclassifiable
NGS	Next Gen Sequencing
ofPMF	overt fibrotic Primary MyeloFibrosis
OS	Overall Survival
PB	Peripheral Blood
pET MF	Post-Essential Thrombocythemia MyeloFibrosis
pfPMF	prefibrotic Primary MyeloFibrosis
PMF	Primary MyeloFibrosis
pPV MF	Post-Polycythemia Vera MyeloFibrosis
PV	Polycythemia Vera
RBC	Red Blood Cell
SM	Systemic Mastocytosis
SM-AHN	Systemic Mastocytosis with an Associated Hematological Neoplasm
SM-MPN	Systemic Mastocytosis with a MyeloProliferative Neoplasm
SSM	Smouldering Systemic Mastocytosis
UMCG	Univerisitary Medical Centre Groningen

Table of Contents

Introduction

MyeloProliferative Neoplasms

MPNs consist of clinic-pathologic entities that showcase overproduction of a variety of blood cells, and therefore form a certain group of blood cancers. Commonly, this overproduction correlates with somatic mutations most often found in specific and usually mutually exclusive gene markers. The major proliferative component in MPNs, and thus the diagnosis and prognosis of the MPN in question, can differ greatly. Affected blood cells range from thrombocytes and erythrocytes up to granulocytes. A distinction can be made between BCR-ABL1-positive MPNs and BCR-ABL1-negative MPNs, the latter category will be focused on in this study. According to the 2016 WHO classification of tumours of haematopoietic and lymphoid tissues (1), MPN can be divided into seven categories, of which the three major subcategories comprise the BCR-ABL1-negative JAK2/CALR/MPL mutation-related MPNs. The other 4 types include CML, which is BCR-ABL1-positive, and CNL, CEL-NOS and MPN-U. The aim for this study will be focused solely on the BCR-ABL1-negative major subcategories, consisting of PV, ET and PMF.

Diagnosis and Classification

Diagnosis of MPNs, and their subtype, is largely based on cytologic analysis and BM biopsy. Presence of a JAK2, CALR or MPL mutation is one of the key criteria to confirm the diagnosis of MPN. Moreover, elevated concentrations of the affected blood cell-type(s) give insight into the specific MPN subcategory and further confirm the diagnosis. In order to form a conclusive and unambiguous diagnosis, close attention has to be paid to the specific blood levels in PB samples and histopathology of BM samples. This is due to overlap of genetic markers and histopathologic phenotype through MPN subtypes. Whereas JAK2 V617F is present in 90% of PV cases, it is found in 70% of ET cases as well. Histopathological abnormalities pointing to combined disease phenotypes may also prove indecisive. In some cases, increased megakaryoblastic as well as erythrocytic proliferation, or a shift from one phenotype to another phenotype over time is found. (2)

Heterogeneity of MPN phenotype is widely influenced by several factors. These include more conspicuous findings like the type of driver mutation and the presence of additional passenger mutations. However, less distinct determinants such as the JAK2 V617F allele burden also play a significant role. Despite a combined significant influence, not all of these potential factors are extensively studied or considered upon MPN diagnosis and classification as of yet. (3)

To elucidate the specific differences and similarities between these MPN subcategories, a clear classification has been made. In the group of JAK2/CALR/MPL mutation-related MPNs, this classification entails the separation of PV, ET and PMF. Through the earlier-mentioned WHO guidelines, the specifications of each of these types can be distinguished and more clearly understood. Diagnostic criteria have been set up to differentiate between each type. An overview of all diagnostic criteria for each MPN subtype is laid out in table 1 below. An overview of the MF grading system is laid out in table 2 underneath.

Table 1: Diagnostic criteria of different MPN subtypes (PV, ET, pfPMF, ofPMF, pPV-MF and pET-MF), according to WHO guidelines. BM fibrosis grading can be found in table 2.

	Major criteria			Minor criteria	
PV	Elevated Hb (>16,5 g/dL in men; >16,0 g/dL in women) or Elevated Ht (>49% in men; >48% in women) or Increased RBC mass (>25% above mean normal predicted value)	BM biopsy showing age-adjusted hypercellularity with trilineage growth (panmyelosis)	Presence of JAK2 V617F or JAK2 exon 12 mutation	Subnormal serum erythropoietin level	
ET	Platelet count ≥ 450 x 10^9/L	BM biopsy showing proliferation mainly of the megakaryocytic lineage, rarely a minor increase in reticulin fibres (grade 1)	WHO criteria for BCR-ABL1-postive CML, PV, PMF or other myeloid neoplasms are not met	Presence of a clonal marker or Absence of evidence of reactive thrombocytosis	
pfPMF	Megakaryocytic proliferation and atypia, without reticulin fibrosis grade >1, accompanied by increased BM cellularity, granulocytic proliferation and (often) decreased erythropoiesis	JAK2, CALR, or MPL mutation or Presence of another clonal marker (associated with myeloid neoplasms, such as: ASXL1, EZH2, TET2, IDH1, IDH2, SRSF2, SF3B1)	WHO criteria for BCR-ABL1-positive CML, PV, ET, myelodysplastic syndromes, or other myeloid neoplasms are not met	Presence of at least one of the following, confirmed in 2 consecutive determinations: - Anemia not attributed to a comorbid condition - Leukocytosis ≥11 x 109/L - Palpable splenomegaly - Elevated Lactate dehydrogenase level	
ofPMF	Megakaryocytic proliferation and atypia, accompanied by reticulin and/or collagen fibrosis grades 2 or 3				Leukoerythroblastosis
pPV-MF	Documentation of a previous diagnosis of WHO-defined PV	BM fibrosis of grade 2-3		Presence of atleast two of the following: - Anemia or sustained loss of requirement of either phlebotomy or cytoreductive treatment for erythrocytosis - Leukoerythroblastosis - Increasing splenomegaly - Development of any 2 (or all 3) of the following constitutional symptoms: >10% weight loss in 6 months, night sweats, unexplained fever (>37.5 °C)	
pET-MF	Documentation of a previous diagnosis of WHO-defined ET				Elevated lactate dehydrogenase level

Table 2: Semiquantitive bone marrow fibrosis (MF) grading system, as included in the WHO classification of MPNs (1)

Grade	Definition
MF-0	Scattered linear reticulin with no intersections (cross-overs), corresponding to normal bone marrow
MF-1	Loose network of reticulin with many intersections, especially in perivascular areas
MF-2	Diffuse and dense increase in reticulin with extensive intersections, occasionally with focal bundles of thick fibres mostly consistent with collagen and/or associated with focal osteosclerosis
MF-3	Diffuse and dense increase in reticulin with extensive intersections and coarse bundles of thick fibres consistent with collagen, usually associated with osteosclerosis

Polycythemia Vera

PV is mainly characterized by a prominent increase of RBCs and is practically always associated with a mutation of either JAK 2V617, or possibly another type of JAK2 mutation usually focused on exon 12. Said mutation may present trilineage expression, and thereby manifest panmyelosis, making it more difficult to diagnose and differentiate. Diagnosis of PV is valid upon confirmation of all 3 major criteria, or the first 2 major criteria plus the minor criterion.

Essential Thrombocythemia

ET primarily involves the megakaryocytic lineage and is therefore closely associated with thrombocytosis in PB and increased numbers of megakaryocytes in BM. Similar to PV, ET is largely connected to a JAK2 mutation, but can also show a mutation of CALR or MPL. The presence of any of these mutations is seen in about 90% of the ET cases. (1) Diagnosis of ET is confirmed when all major criteria, or the first 3 major criteria and minor criterion are met.

Primary MyeloFibrosis

PMF is primarily characterized by proliferation of abnormal megakaryocytes and granulocytes in BM, usually resulting in reactive deposition of fibrous connective tissue and extramedullary hematopoiesis upon progression. There is a clear deterioration noticeable in the progression of PMF, diagnosis is therefore distinguished for the separate stages that occur. The prefibriotic (early) stage has different criteria to be met than the overt fibrotic stage. Since common mutations of PMF are shared between the other discussed MPNs, analysis of bone marrow morphology is paramount in distinguishing any phase of PMF.

Prefibriotic PMF is predominately characterized by hypercellular BM with absent to minimal reticulin fibrosis. This early stage of PMF is prone to go by undetected due to the relatively mild symptoms, usually solely discovered through hypercellularity of mostly neutrophils and atypical megakaryocytes in a BM biopsy. The latter, and more specifically its morphological atypia and topographical distribution, is essential for diagnosing this stage. Diagnosis of prefibriotic/early PMF is conclusive upon confirmation of all 3 major criteria and at least 1 minor criterion.

Overt fibrotic PMF is, due to progression, expressed more prominently, and has more severe symptoms such as marked reticulin or collagen fibrosis in BM, often accompanied by osteosclerosis. Diagnosis of overt fibrotic PMF is conclusive upon confirmation of all 3 major criteria and at least 1 minor criterion.

Simultaneously occurring MPNs

Alongside the previously mentioned types and stages of MPN, there is also the possibility of a somewhat concurrent occurrence of MPNs. Both PV and ET can progress into myelofibrosis, thus showcasing PV/ET and a type of PMF simultaneously. These conditions are termed as post-PV myelofibrosis and post-ET myelofibrosis. One approach of describing events like these, is considering them to be a more deteriorated version of the original MPN. In addition to this.

Post-PV MF has been found to be the cause of around 20% of diagnosed PMF cases. Post-ET MF however, only occurs about half of the time as compared to Post-PV MF. Additional focus has to be laid on Post-ET MF cases and its diagnostic criteria, to not be confounded with pre-PMF with tendencies of thrombocytosis. This is largely due to the fact that complications and expected survival are widely dissimilar in the latter.

The possibility of transition from either PV or ET to a PMF-like state, endorses the hypothesis that MPN can be viewed as a spectrum of disease, rather than a clear separation between each type.

Prognosis

As mentioned earlier, MPN can be viewed as a spectrum of subtypes and severity. To elucidate differences in median OS, various previous research has been combined in a meta-analysis. OS ranges in ET and PV were established through a cohort of 3023 patients (median age 62 years; 665 PV, 1076 ET and 1282 PMF according to WHO-criteria), in which median OS was found to be 18 years for ET and 15 for PV. (4) Furthermore, data was combined with research in a cohort of 826 patients, of which 58% were followed until death. Median OS was found to be 19,8 years in ET and 13,5 in PV. (5)

For determination of OS in both PMF stages, a cohort of 278 pfPMF and 383 ofPMF patients was studied, showing a median OS of 17,6 and 7,2 years for pfPMF and ofPMF respectively. (6) Patients were diagnosed in accordance with WHO-criteria.

To establish median OS in pET-MF and pPV-MF, and to further assess OS in ofPMF, a cohort consisting of 1099 patients diagnosed with MF according to 2008 WHO criteria was studied. Of these patients, 755 were diagnosed with PMF, 181 with pPV-MF and 163 with pET-MF. Median OS for pPV-MF, pET-MF and PMF was 73, 48 and 45 months respectively. (7) Distinction between ofPMF and pfPMF was not yet made in the classification used here, the median OS of found here therefore might include pfPMF cases as well. This seems unlikely however, upon considering the earlier mentioned median OS of 7,2 years for ofPMF specifically.

Further assessment of OS in pET-MF and pPV-MF was made using research on a cohort of 685 patients with a secondary MF. (8) Median OS in pET-MF patients (n = 333) concluded to be 14,5 years. In patients with pPV=MF (n = 352), median survival was 8,1 years. Diagnostic criteria established by the IWG-MRT were used for review. (9)

Median OS in MDS patients was determined using a study in a cohort of 2754 patients. Average OS was estimated at 3,3 years, combining median OS of all prognostic subgroups. (10) Cohort comprised of patients with primary MDS only, diagnosed with WHO-criteria.

Average median OS in AML was ascertained in a cohort of 357 patients newly diagnosed with AML and the FLT3 mutation and proved to be around 2,1 years. (11) A better insight would be acquired if all AML subtypes were included, as well as most common mutations. However, through this study the severity of AML is illustrated quite well, and it finds support in various other research. (12)

To assess median OS in SM-MPN, a cohort of 138 SM-AHN patients was studied. In this cohort, 55 patients were diagnosed with SM-MPN, and showed a median survival of 2,6 years. (13) However, KIT D816V mutation was only found in 52% of cases, suggesting that this cohort might contain a high frequency of more progressed forms and thus lowering median OS. Moreover, SM- and MPN-subtypes of this subgroup are not fully classified, rendering the average median OS of SM-MPN ambiguous. Seeing as the selected cohort might not be representative of actual SM-MPN, it is expected that actual median OS of SM-MPN is slightly longer, indicating a more favourable prognosis and outcome than depicted here.

An overview has been made to showcase the progression and implications on median overall survival time, as visible in figure 1 below. When solely comparing median overall survival times a trend becomes apparent, in which progressed forms such as MDS, AML and progression to MF have a significantly worse prognosis. While this gives some idea of the individual implications of each subtype, it by no means renders a complete picture. However, the obtained trend as seen here greatly overlaps with other prognostic factors and hypotheses.

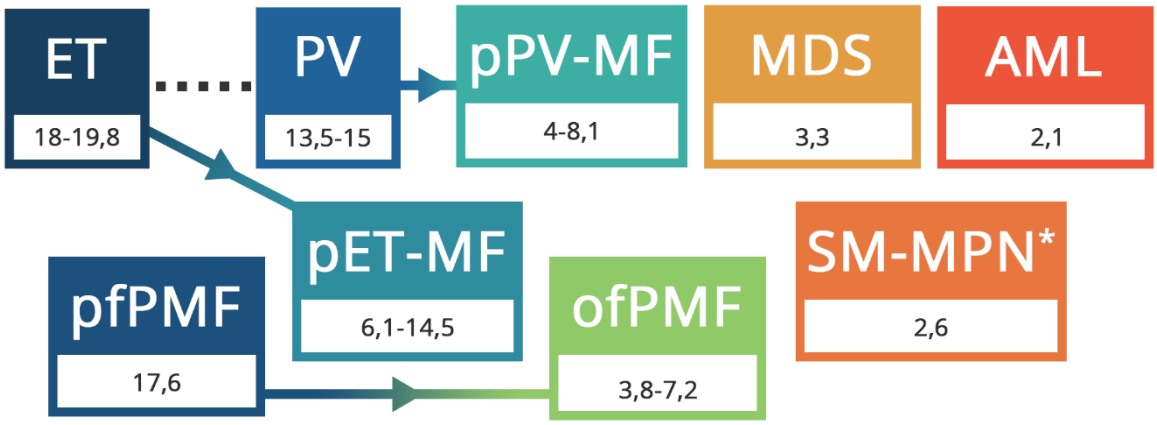

Figure 1: An overview of the possible progression and transformation of MPN, and the implications on median overall survival time in years. Dotted lines represent transformation, colored lines represent progression between specific subtypes. Overall progression to MDS, AML or SM-MPN is possible from all subtypes. The median overall survival times have a range of 18-19,8 years in ET (14); 17,6 years in pfPMF (15); 13,5-15 years in PV (14); 6,1-14,5 years in pET-MF (7, 8); 4-8,1 years in pPV-MF (7, 8); 3,8-7,2 in ofPMF (7, 15); 3,3 years in MDS (16); 2,6 years in SM-MPN (35) and 2,1 years in AML (12). *Median OS found in SM-MPN might be biased due to lack in cohort representativeness and is expected to be slightly longer.

Polycythemia Vera

PV has evident impact on bone marrow and blood, the lifetime prevalence of an episode of arterial or venous thrombosis is 20% in patients with diagnosed PV. (1) Generally, survival times transcending 10 years have been stated, with an overall average surpassing 13 years (1, 14). Patients aged <60 have an average survival time of 24 years, showcasing the influence of old age as a prognostic factor. Common causes of death include mainly thrombotic complications and second malignancies. Noteworthy is the number of patients that further deteriorate to myelodysplastic syndrome or blast phase/acute myeloid leukemia, scaling up to 20%. (1)

Post-PV MyeloFibrosis

This deteriorated stage is characterized by overt reticulin and collagen fibrosis In BM, as seen in the diagnostic criteria. A shift to leukocytosis as a result of the progression to Post-PV MF often correlates with a more aggressive course of the disease. (1) Survival times in Post-PV MF are significantly worse as compared to PV without progression. Several studies have found a median overall survival time between 4-8,1 years. (7, 8)

Essential Thrombocythemia

As expected with any MPN, the bone marrow and blood are the main sites of impact. ET can, similar to PV, cause splenic or hepatic vein thrombosis (1) ET is mainly asserted as an indolent illness with long asymptomatic intervals, even though interferences of potentially lethal breaks of thromboembolic or haemorrhagic episodes can arise. As a result, life expectancy is near normal and survival times transcending 10-15 years. Median survival times range from 18-19,8 years in multiple studies. (14) This can be partially explained by the fact that ET more often than not occurs late in middle life. (1) Seeing as ET is more often than not asymptomatic, most cases are discovered on routine checks. Therefore, actual median OS might be longer than depicted here.

Post-ET MyeloFibrosis

Just as seen in PV cases, ET can deteriorate into PMF-like symptoms, such as severe bone marrow fibrosis. Although happening more sparingly, with a life-time prevalence of just 10% in ET-diagnosed cohorts. Progression to MF affects median survival times greatly and reduces the range to 6,1-14,5 years. (7, 8)

Primary MyeloFibrosis

As mentioned earlier, there is a clear distinction to be made between the different stages of PMF. Ultimately, it can be divided into prefibrotic PMF and the further progressed overt fibrotic PMF. Around 30% of PMF cases are expressed asymptomatically and are detected during routine check-ups when symptoms like splenomegaly or aberrant blood counts, due to anemia, leukocytosis or thrombocytosis, are found.

Prefibriotic PMF has a relative survival rate of approximately 10-15 years (1), although median survival times around 17,6 years have also been witnessed. (15) When compared to most other MPN types, overt fibriotic PMF surpasses in terms of severity. This is evident from the median survival time of 3,8-7,2 years. (1, 7, 15) Median OS in pfPMF is significantly longer than survival times seen in ofPMF, underlining the substantial differences between both phases.

Mutations found in MPN

Mutations

As described earlier, the JAK2 V617F mutation occurs as a gain-of-function point mutation. It is an exon 14 G to T somatic mutation with a nucleotide change at position 1849, substituting valine to phenylalanine at codon 617. The JAK2 mutation has been described in various myeloid neoplasms, but particularly in the MPN types discussed here. The allele burden of JAK2V617F has shown to influence the phenotype of MPN greatly, both in mouse models as well as studies. (17) A lower expression of JAK2 showed a tendency for an ET phenotype, whereas a normal or higher expression displayed PV with or without thrombocytosis respectively. Other studies have shown the same tendency towards an ET phenotype with lower allele burdens of JAK2 as compared to PV or PMF associated with higher allele burdens. A homozygous state of JAK2V617F, as opposed to a heterozygous state, correlates with an increased hemoglobin level, leukocyte count, a lower platelet count and pruritus. This is largely similar to the phenotype acquired with a higher allele burden of JAK2.

CALR is located in the lumen of the endoplasmic reticulum, here it functions as a chaperone. Additional functions include calcium signaling and protein quality control. CALR is able to control calcium homeostasis, through calcium buffering activity of its C-terminal domain. Mutations in CALR occur as a +1 base pair frameshift in the last coding exon (exon 9). (18) Mutant CALR can bind to the thrombopoietin receptor MPL to activate JAK-STAT signaling. CALR mutations are classified into type 1, type 2 and residual type 3 mutations. Type 1 (52-bp deletion) and type 1-like mutations account for roughly 65% of CALR mutations. Type 2 (5-bp insertion) and type 2-like mutations account for 32%. The residual type 3 accounts for the remaining 3% of CALR mutations. (18) Type 1 and type 1-like CALR mutations show a closer association to PMF rather than ET. Furthermore, they show an increased risk of myelofibrotic transformation when they do occur in ET. On the contrary, type 2 and type2-like CALR mutations occur predominantly in ET rather than PMF. When a type 2 or type2-like CALR mutation is present in PMF however, it often shows a worse prognosis compared to type 1 and type1-like mutations. (18, 19)

Like JAK2, the MPLW515L mutation occurs as a gain-of-function point mutation. MPL belongs to the hematopoietin receptor superfamily and is responsible for enabling the ligand thrombopoietin. Through this mechanism, it promotes hematopoiesis as well as megakaryocyte growth and differentiation. (17) The MPLW515L mutation consists of a G to T transition at nucleotide 1544, substituting tryptophan to leucine at codon 515. Another MPL mutation at the same codon was discovered incidentally, MPLW515K. Both MPLW515L and MPLW515K have shown close association with MPNs. Other somatic MPL mutations that have been linked to the MPN subtypes comprise MPLW515S and MPLS505N, which both share higher prevalence rates than the aforementioned MPL mutations. Whereas the MPLW515L/K mutation has a prevalence of roughly 5% in PMF and 1% in ET (17), the others show a prevalence of up to 11% in PMF and 4% in ET. It has been suggested that MPL mutations incline towards myeloid proliferation and differentiation, whereas JAK2 mutations tend to be associated mostly with the erythroid lineage. Furthermore, MPL-positive PMF and ET patients were shown to carry an older age and more anemic tendencies compared to MPL-negative cases.

It has been elucidated before, that the 3 biomarkers (JAK2, CALR and MPL) have a significant impact on clinical outcomes. There also is a substantial difference in mutant allele burden between said genetic lesions. Whereas CALR-positive ET patients only sporadically carry mutant allele burdens >75% (20), it is commonly found that JAK2-mutated MPNs have incredibly high allele burdens. Previous research indicates that a mutation in any of the aforementioned genes alone can initiate MPN, supported by additional mouse models. Additionally one of these mutations is the sole aberrant gene in about 50% of MPN patients. Distribution of the driver mutations can be found in figure 2 below.

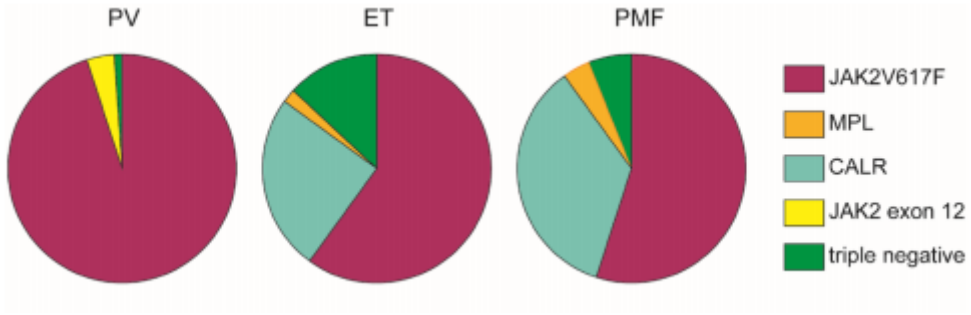

Figure 2: Distribution of common driver mutations JAK2617F, MPL, CALR and JAK2 exon 12 in PV, ET and PMF. Frequency of triple-negative cases within each MPN phenotype is shown as well. (21)

Genomics in PV

Since the JAK2 mutation is virtually always present in PV, a distinction between JAK2-positive and JAK2-negative cases cannot be made. However, a higher allele burden of the JAK2V617F mutation is associated with PV. (22) Moreover, JAK2-mutated MPNs in general show a tendency towards phenotypes similar to PV, indicating their influence.

Genomics in ET

The JAK2 mutation is mostly associated with prominent leukocytosis, lower platelet levels and a higher risk on thrombotic complications and transformation into PV. (23) Poor prognosis is mostly associated with JAK2-mutated or triple-negative cases. JAK2V617F-mutated cases showed an increased risk of thrombosis as compared to CALR-mutated patients. (24) Findings like these suggest that JAK2 can be considered as the most thrombogenic driver mutation in MPN.

MPL-mutated cases are quite rare, as seen above, with an incidence less than 5%. (25) These patients often have an older age, lower hemoglobin levels and a higher rate of progression to MF. In MPL-unmutated ET the progression rate is 7,5%, whereas in MPL-mutated cases the rate is 33,3%. (25) These findings indicate that potentially, some MPL-positive ET patients might actually have pfPMF instead.

ET-patients with the CALR mutation commonly have a younger age, lower hemoglobin/leukocyte counts, compared to the other driver mutations. Contrary to seen in JAK-mutated ET patients, CALR-mutated cases have increased platelet counts and an increased risk of transformation to PMF. In terms of CALR-subtype, type 2-mutations are found to have the more indolent course as compared to type-1 like mutations. (23) Although the presence of a type 2-like mutation showed association with higher platelet counts, there was a lower risk of thrombosis. (19) This difference was even more significant when comparing CALR mutations to JAK2V61F-mutated cases.

Genomics in PMF

In PMF, JAK2- and MPL-mutated cases show no significant difference in prognosis or outcome. (26, 27) The JAK2V617F mutation occurs less frequently in PMF as compared to other MPN subtypes. MPL-mutations on the other hand, are most frequently found in PMF. This is in line with the aforementioned increased risk of transformation to PMF, in ET.

CALR-positive patients have a more indolent course and better overall survival than patients carrying the JAK2 or MPL mutation. (19) This is illustrated by the substantially lower cumulative incidence of both anemia and thrombocytopenia in PMF patients with the CALR mutation. (26) CALR-positive PMF patients generally are considerably younger of age and present a lower leukocyte count and higher platelet count than patients with other driver mutations. (23) This difference in age might contribute to a more favorable outcome. Upon considering the overall survival in PMF, it has been elucidated that patients carrying the CALR-mutation have a median OS of 17,7 years, as compared to 9,2 and 9,1 years for JAK2- and MPL-mutant patients. (26)

Influence of order and number of mutations acquired in MPN

Apart from the type, and subtype, of mutation in MPN, the order of acquirement of such mutation also seems to influence the disease phenotype significantly. CALR and MPL mutations for example, are shown to arise earlier than passenger mutations such as NRAS, TP53, PPM1D and NFE2. (22) When there are multiple mutations present, TET2 and DNMT3A for example, the JAK2 V617F mutation is often the secondary event in ET patients, but an early event in PV- or PMF patients.

Furthermore, a higher number of passenger mutations in a patient is closer associated with PMF as compared to PV or ET. (22) An increase in this number following the age of the patient has been witnessed and the acquired driver mutations also correlate with several hematologic variables. Besides roughly separating PMF from PV or ET, the distinction between ET and PV is also strongly determined by these acquired driver mutations. An increased JAK2 V617F allele burden correlates with increased odds of PV (odds ratio 9,1; P<0,001), as do older age and male sex. (22) Although these driver mutations give some insight into the MPN phenotype and the specific prognosis, it can hardly be considered conclusive. Many different known and unknown factors play a role in the overall outcome, showcasing the request for more personal prognostic models.

In ET, driver mutations have not been shown to affect overall survival; instead, JAK2 mutations have been associated with an increased risk of thrombosis and MPL mutations with an increased risk of transformation into post-ET MF. (28)

Systemic Mastocytosis

Mastocytosis is caused by neoplastic proliferation of mast cells that sequestrate in one or more organ systems, often characterized by an abnormal mast cell infiltrate. In SM, hematological abnormalities can arise, such as anemia, leukocytosis, neutropenia, thrombocytopenia or the more commonly found eosinophilia. Systemic mastocytosis can be differentiated into several types, such as ISM, SSM, SM-AHN, ASM and MCL. (1) In this study we will focus on ISM, and advSM which comprises of the remaining types. SM is diagnosed according to the WHO guidelines, based on major and minor criteria. Presence of multifocal dense infiltrates of mast cells detected in BM sections is a major criterion, whereas minor criteria revolve around morphology, immaturity and CD25 expression of mast cells. Another minor criterion is detection of the KITD816V mutation, which is virtually inseparable from SM diagnosis. (29) To indicate organ involvement and dysfunction, B-findings and C-findings are used. B-findings are commonly related to disease burden, whereas C-findings associate with cytological involvement.

ISM is generally considered to be the least severe variant of SM. When ISM is diagnosed and no such mutation can be detected, the KIT gene should be sequenced, as another type of mutation could be present. ISM is characterized by a low mast cell burden and no cytological involvement.

AdvSM is associated with a higher burden of disease and more prominent symptoms. In advSM, the KITD816V mutation is customarily detectable in several myeloid lineages or even in lymphocytes, illustrating multilineage involvement. (1) Apart from this, cytological involvement is prone to occur as well. Within this subgroup, the focus will be laid on SM-AHN in this study.

The KITD816V mutation

KIT is located at chromosome 4q12 and comprises a class III receptor tyrosine kinase. (17) KIT is most prominently expressed by mast cells, but also hematopoietic stem cells, germ cells, melanocytes and Cajal cells of the GI tract. Among several other responses, KIT signaling shows influence on the JAK-STAT signaling pathway, as seen before with JAK2 and MPL mutations. The KIT mutation consists of a point mutation at the kinase domain at codon 816, with nucleotides 2467-2469, substituting GAC for GTC, and has thus been named KIT D816V. The presence of the notable KITD816V mutation has been described in various cases of SM, especially in ISM variants, (30) other KIT mutations have also shown presence although to a lesser extent.

Mutations other than KIT are found in advSM as well, including TET2, SRSF2, ASXL1, RUNX1, JAK2 and RAS.

Effect of Molecular Genetics

Even in SM, additional mutations besides the prominent KIT D816V mutation have shown presence and prognostic impact. Especially in more aggressive forms of SM, there is a clear correlation between the clinical behaviour and the number and type of additional mutations. Just as seen in MPN, a larger number of additional mutations is associated with a lower overall survival. Furthermore, less aggressive forms of SM like ISM seem less likely to have additional mutations than their more aggressive forms. (31)

Additionally, other research has suggested a strong correlation between the allele burden of KIT D816V with disease activity, disease subtype and overall survival. (30, 32) For example, advSM patients showed a significantly higher KIT D816V allele burden than patients diagnosed with ISM. Furthermore, influence on disease activity was represented by a strong correlation with serum tryptase levels. (30)

Systemic Mastocytosis with an Associated Hematologic Neoplasm

Diagnosis and Classification

As shortly mentioned earlier, one of the main variants of SM is SM-AHN. This diagnosis meets both the criteria for SM as well as any AHN. The AHN component can consist of a myeloid/lymphoid malignancy, although it usually comprises a myeloid disease of non-mast cell lineage, such as AML, MDS, MDS/MPN or MPN. In most cases, AHN is considered to be a secondary neoplasm, although it holds significant clinical and prognostic implications. (1) A hematologic neoplasm like mentioned here, occurs in about 30% of patients diagnosed with SM. Interestingly, the KIT mutation that has distinguished most of the SM types is not only present in the SM section but is also found in AHN cells in the majority of cases. (33, 34) This finding may implicate more similarities in the etiology of SM and its AHN than previously thought.

Diagnostic criteria are solely based on the simultaneous presence of both individual criteria for SM and any AHN. Noteworthy however, is the ineffectuality of serum total tryptase levels in this specific SM for diagnostic purposes. Where in most cases of SM a serum total tryptase level that consistently exceeds 20 ng/mL is a clear minor criterion and valid method for evaluation and monitoring, it is not a valid parameter in SM-AHN.

Prognosis

As previously discussed, SM is generally associated with somatic gain of function point mutations within KIT, more specifically at KIT D816V. (35) KIT (CD117) is expressed by, among others, mast cells and hematopoietic progenitor cells. It therefore plays a significant role in the development of mast cells as well as hematopoiesis and several other processes. Mutated tyrosine kinase is able to promote progression and clonal proliferation, which is reflected in both SM and MPN. Noteworthy is the relatively high level of cell surface KIT expression in mast cells compared to other cell lineages that share KIT expression. Additionally, the allele burden of the KIT mutant seems to be closely associated with the burden of neoplastic mast cells, and thus prognosis and survival. (34)

In researched cohorts, exhibition of eosinophilia was often found, especially in SM-MPN patients. The presence of such eosinophilia however, did not prove to substantially influence the clinical outcome in these patients. (35) Median survival times in SM-AHN appear to last around 24 months, of which SM-MPN patients usually hold a median survival of 31 months. This is significantly higher than the other aforementioned types SM-CML and SM-MDS which show a median survival of 15 months and 13 months respectively.

SM-AHN is considered to be the second most frequent subtype of SM, following ISM. (36, 37) SM in SM-AHN can consist of either ISM or advSM, the AHN component usually consisted of an associated myeloid neoplasm such as CML (22%), MDS (13%) and MPN (28%), of which the latter predominated. (37) In this study, focus will be laid on SM-MPN, in which the MPN component can comprise ET, PV, PMF or pPV- and pET-PMF.

Co-occurrence of JAK2 V617F and KIT D816V mutation in SM-AHN

The JAK2 V617F- and KIT D816V mutation have been shown to occur concomitantly in various previous research. (17, 38) Moreover, in patients with co-occurrence both mononuclear and polymorphonuclear cells were positive for both the JAK2 and the KIT mutation, showcasing simultaneous presence in PB cells. (39) As mentioned earlier, the JAK2 V617F mutation plays a key role in the MPNs discussed here. Even more interesting however, is its role in SM-AHN. Research suggests a possibility of the JAK2 V617F mutation in ISM resulting in an increase in the risk of progressing into advSM. (40) Findings like these reveal the possible multilineage involvement that the JAK mutation brings and strengthen the connection between JAK and KIT mutations and their shared clinical picture.

Treatment of MPN component

The AHN component in SM-AHN is usually the prime target for treatment and is proven to be more treatment sensitive, reaching complete remission in all SM-AHN patients (n= 38). (35) As a result of the JAK2 mutation playing the prominent role in the most common MPN subtypes, a potential treatment for MPN patients in general consists of JAK2 inhibitors. Previous research has shown that JAK2 inhibitors can also excel in patients with the MPL(W515) mutation, found in a significant number of JAK2-negative cases. (41) More recent studies have shown that ruxolitinib, a JAK2 inhibitor, has a similar efficacy over all three well-known and previously described MPN mutations. Another treatment comprises IFN-α, which has shown promising efficacy in both Jak2V617F-positive HSCs as well as in CALR-positive MPN patients. A higher percentage of nonresponse was found in CALR-positive patients. It became evident that myeloid cell lines expressing CALR mutants need a dose of IFN-α that is more than 5 times higher as compared to JAK2 mutant cells. An explanation to this is formed by a IFN-α sensitization, caused by the JAK2 mutation. It seems that IFN-α as a treatment shows more potency in JAK2V617F-positive cases, as opposed to CALR-positive cases, through their mechanism and role in the JAK-STAT signaling pathway. (42)

Little is known about the implications KIT mutations have in MPN. Due to the evident impact the type of driver mutation has on prognosis, outcome and treatment of MPN, it seems essential to further assess the influence of KIT D816V. Similar as seen in JAK2, CALR or MPL-mutated cases, presence of a KIT mutation could affect treatment greatly.

Droplet Digital PCR

In this study, ddPCR has been used for detection and quantification of the KITD816V mutation in patients diagnosed with MPN. Using ddPCR instead of the previously conventional qPCR brings several advantages. In terms of variability, qPCR seems to be lacking behind severely. The variance between replicate samples with a slightly inconsistent RT mix contaminant showed to be 60-87% for qPCR, whereas ddPCR had only 7-30%. (43) Because of the necessity of standard curves, among other factors, qPCR is less precise and reproducible. Additionally, ddPCR has the advantage of direct, absolute and quantitative analysis with a high sensitivity through thousands of droplets that each mimic an individual PCR well. (44) Furthermore, ddPCR has an end-point measurement and therefore is not dependent on reaction efficiency, which is especially useful with targets of low abundancy. (43) This is strengthened by a study from Waterhouse et al. in which in 14% of the samples, the JAK2 V617F mutation could only be detected by ddPCR. All of these were follow-up samples shortly after allogeneic stem cell transplantation, and thus low abundant targets. (45)

Aim & Hypothesis

The aim of this study is to investigate the concomitant occurrence of the KITD816V mutation in BCR-ABL1-negative MPNs. To further elucidate this interaction, several essential aspects will be considered. Prevalence will be studied in a selected cohort of MPN patients, harboring the JAK2 V617F, MPL or CALR mutation. Clinical outcome and implications of all intern UMCG patients will be reviewed and differences between MPN and SM-MPN will be further laid out.

Recently, Craig et al. found a 5,8% prevalence of SM in BCR-ABL1-negative MPNs, with NGS. (29) Based on previous research, the assumption is that in low abundant targets the KIT D816V mutation might not be properly detected with less sensitive methods like NGS, or even qPCR. We therefore hypothesize that the actual prevalence is significantly higher and will be approximated more closely with ddPCR. Moreover, the clinical implications this overlap could bring have yet to be fully explored. Multiple case reports have been done on the clinical presentation and outcome of SM-MPN (46, 47), but these were focused on individual cases rather than a general trend. Our aim is to apply similar investigations on a larger cohort, to reveal more extensive differences.

Material & Methods

Patient selection

A cohort of BCR-ABL1-negative MPN patients, determined with either the JAK2 V617F, MPL or CALR mutation in the UMCG, was selected. Patients with PB or BM samples between 2016 till 2020 were included and a ddPCR assay has been carried out on all available samples. Patient characteristics were gathered using a laboratory information system and are laid out in Appendix 1.

A subgroup was made of patients receiving treatment within the UCMG, intern patients. This cohort was further investigated on clinical implications with help of an electronic health record, a summary and overview can be viewed in Appendix 2. In addition to diagnosis and general data, the course of disease, and thus the progression, has also been examined.

Sample preparation

Leukocytes were isolated from BM and PB samples according to SOP ("Leukocyten isolatie t.b.v. moleculair biologisch onderzoek" Documentnr.: 06332) to acquire DNA. Erythrocytes from patient material were lysed using ammonium chloride and resuspended in PBS. DNA was isolated from this resuspension according to SOP ("DNA-isolatie: Handmatig en m.b.v. de QIAcube" Documentnr.: 06385). Using protease and a lysis-buffer (AL-reagens), DNA was extracted. Afterwards, DNA was precipitated with ethanol on QIAmp filter column, washed and dissolved in AE-buffer. Concentrations of dsDNA were measured with NanoDrop 2000, samples were further diluted to 50 ng/µl.

ddPCR reaction and analysis

The ddPCR reaction was performed according to SOP ("Het uitvoeren van een ddPCR analyse" Documentnr.: 43737), tailored for KIT D816V detection in DNA, identical for both BM and PB samples. The reaction mix consisted of ddPCR supermix for probes (no dUTP), Primer/probe mix for KIT p.D816V DNA, HindIII-HF buffer and DEPC-treated water. On a 96-well plate, each well was filled with 15,5 µL reaction mix and 9,5 µL DNA.

Using a Bio-Rad QX200 Droplet generator, droplets of the mixture were generated according to SOP ("QX200 Droplet Generator/Reader.: 42608). On a DG8 cartridge, 20 µL of sample mixture was transported from each well to the corresponding place. After addition of 70 µL Droplet Generation Oil, the droplets were generated and 40 µL was transported to a new 96-well PCR plate. Hereafter, the plate was sealed using a PX1 PCR plate sealer.

The PCR reaction was executed using a C1000 Touch Thermal Cycler and conditions were set according to the protocol in table 3 below. A gradient of steps was used to achieve the appropriate stages, in the order depicted in table 3.

Table 3: PCR protocol for KIT p.D816V DNA assay. Sample volume was 40 µL, Lid temperature 105 °C and PCR ramp rate 2°C/sec.

Stage		Temp. °C	Time (h:mm:ss)	
Enzyme activation		95	0:10:00	
PCR	Denaturation	94	0:00:30	40 cycli
	Annealing/Elongation	58	0:01:00	
	Enzyme deactivation	98	0:10:00	
Cooling		4	Infitine (hold)	

Upon completion of PCR amplification, the plate was analyzed using a QX200 Droplet Reader. The FAM channel was used for mutant fluorescent detection and the HEX channel for WT detection. Results were processed and reviewed using QuantaSoft Analysis Pro. As a positive reference, HMC1-2 samples were used. For negative references, healthy BM samples, TE buffer and reaction mix were used.

Samples were reviewed manually and declared positive when three or more positive droplets were consequently detected in both wells. Attention has been laid on the similarity in amplitude of said droplets, as compared to the positive control. Additionally, mutant DNA concentration had to exceed the LOD and concentration of negative controls. After a correction for the random distribution of droplets using the Poisson algorithm, Copies per µL and VAF% were calculated.

Due to low abundant targets and accessory ambiguity, some samples have been retested. Out of the total 369 samples, 123 were deemed inconclusive at first. A distinction has been made between uncertain (low abundant), technically inferior and single-positive results. Additionally, some samples were re-tested for proper quantification. Uncertain outcomes were bordering on limit of detection or had positive droplets at a relatively low amplitude and were re-tested. Technically inferior results generally showed an inadequate amount of total droplets (<10000), little to no WT-positive droplets, or major shifts and were therefore re-tested as well. Single-positive samples were characterized by one single-positive droplet, often at a significantly high amplitude. There were 50 KIT-inconclusive, mostly single-positive samples but, apart from one, they have not been re-tested in the scope of this study. Of the remaining 73 re-tested samples, 11 were deemed positive conclusively. Because this group mainly consisted of low-abundant targets, 7 of these were considered to be weak positive, 5 of which with an uncertain analytical result. The 1D spectra of these samples can be found in Appendix 3.

Diagnostic Scoring

In order to classify diagnoses and investigate clinical implications, a diagnostic scoring system has been set up. Distinction of scores was based on current conceptions of overall survival, progression of disease and disease burden to estimate severity. In table 4 below, the scoring table used here has been laid out.

Table 4: Scoring table used to differentiate diagnoses of intern patients in this cohort. The higher the score (A – R), the higher the implied severity of disease.

Diagnostic Score	Conclusive Diagnose
A	No SM or MPN conclusively diagnosed
B	Strong suspicion of either SM or MPN
C	Only SM conclusively diagnosed
D	SM with MPN suspicion / MPN with SM suspicion
E	ET
F	PV
G	ET/PV overlap
H	ET + MF grade 1
I	PMF (prefibriotic)
J	PMF grade 2-3 (overt fibriotic)
K	Post-PV-MF grade 1 | Post-ET/PV-MF grade 1
L	SM-MPN
M	SM-MPN + MF grade 2-3
N	Post-PV/ET MF grade 2-3
O	MDS or CML
P	MDS/CML + MF grade 2-3
Q	AML
R	AML + MF grade 2-3

As visible above, almost no diagnoses overlap in diagnostic score. Apart from the occurrence of either MDS or CML (with or without MF grade 2-3), the overlap of PV and ET in some patients, or overlapping suspicions of either MPN or SM, all diagnostic scores account for a unique diagnosis. This has been a conscious choice as present research and knowledge do not succeed in an unambiguous differentiation on this level. Within each diagnosis, many factors may contribute to burden of disease and/or progression. Thus, a higher diagnostic score does not necessarily equal a poorer clinical outcome. The scoring table depicted above therefore only contributes a general trend in diagnoses of our cohort.

Results

KIT D816V Mutation

In total, 320 unique patients and 369 samples have been tested. The cohort consisted of 254 patients harboring JAK2 V617F, and 66 CALR-positive patients. In table 5 a summary of the results has been laid out. An overview of all tested samples and patients can be found in Appendix 1.

Table 5: Overview of the results of the KIT D816V ddPCR assay, showcasing number of patients with either JAK2 or CALR mutation and corresponding percentage (%).

N=320	JAK2 V617F	CALR
KIT-Postive	27/254 (10,6 %)	2/66 (3,0 %)
KIT-Inconclusive	35/254 (13,8 %)	9/66 (13,6 %)
KIT-Negative	192/254 (75,6 %)	55/66 (83,3 %)

Moreover, prevalence of JAK-positive patients was compared with patients positive for CALR-mutations. Results indicate a favour towards JAK2-mutation in KIT-positive patients, seeing as 93,1% of KIT-positive patients were harboring this mutation. Compared with the total cohort, in which 79,4% of patients had a JAK2 V617F mutation, the bias towards JAK2-mutated patients seems significant. A similar distribution of mutation genes was found in the negative subgroup, with a prevalence of 78,0% for JAK2-mutated patients. This inclination is underlined by the increased prevalence of JAK2/KIT-positive patients, as compared to the total prevalence of KIT-mutations.

KIT D816V-positives

The characteristics of all the KIT-positive samples are shown in table 6 below, 1D spectra of these samples can be found marked in Appendix 3. Patients were sorted based on number of copies per µL and patients with a KIT D816V mutation of uncertain clinical significance were marked orange. Diagnose at time of sample collection has been listed as well, in some cases mastocytosis was already expected or diagnosed.

Table 6: Characteristics of KIT D816V-positive samples, with corresponding diagnosis, MPN mutation type, sample type, copies per µL, VAF% and number of positive mutant events.

Patient	Sample#	Diagnosis	MPN Mutation	KIT previously detected	Sample type	Copies/µL	VAF%	# positive mutant events
P1	19-2170	SM-PMF	JAK	Yes	PB	822,45	18,135239	14364
P2	18-0273	SM-MPN + MF2-3	JAK	Yes	PB	733,98	15,018390	16518
P3	16-1889	MPN	CALR	No	PB	26,20	0,617810	744
P4	19-1290	ISM + PMF suspicion	JAK	Yes	PB	24,18	0,337440	754
P5	19-1563	SM-ET/PMF	JAK	Yes	PB	21,26	0,368369	629
P6	17-0526	MPN	JAK	No	PB	15,84	0,312090	364
P7	19-2478	SM	JAK	Yes	PB	3,02	0,055733	100
P8	16-1353	MPN	JAK	No	PB	2,01	0,053415	45

P9	19-2552	MPN	JAK	No	PB	1,33	0,027484	30
P10	16-0259	Trombocytosis / MDS	JAK	No	PB	1,23	0,035860	33
P11	19-0939	Leukocytosis	JAK	No	PB	1,22	0,027787	31
P12	17-0877	ISM	JAK	Yes	PB	1,10	0,022753	19
P13	19-2180	Erytrocytosis/ trombocytosis	JAK	No	BM	1,06	0,026860	24
P14	19-2896	MDS/CMML	JAK	No	PB	0,91	0,015420	22
P15	17-0014	SM-MPN + MF2-3	JAK	Yes	PB	0,79	0,019680	20
P16	19-2857	AML + MF2-3	JAK	No	PB	0,58	0,009590	12
P17	18-0849	MPN	JAK	No	BM	0,51	0,013998	13
P18	19-2504	ISM	JAK	Yes	PB	0,42	0,010357	14
P19	16-0108	MPN	CALR	No	PB	0,39	0,009030	6
P20	20-0762	ET	JAK	No	PB	0,31	0,002906	8
P21	19-0334	PV	JAK	No	PB	0,25	0,005336	6
P22	19-2753	ET	JAK	No	PB	0,25	0,004900	6
P23	19-0763	ET	JAK	No	BM	0,23	0,005066	5
P24	18-2459	MPN	JAK	No	PB	0,22	0,005088	5
P25	20-0442	SM-MPN	JAK	Yes	BM	0,20	0,003023	5
P26	17-1802	MPN	JAK	No	PB	0,17	0,003809	9
P27	16-0950	PMF	JAK	No	PB	0,11	0,003130	4
P28	20-0175	MPN	JAK	No	PB	0,11	0,002812	4
P29	18-1838	MPN	JAK	Yes	PB	0,08	0,002114	2

In Appendix 4, figures 3-31, the 2D spectra of the ddPCR assay from each patient are laid out. Only the samples with adequate technical quality and quantification were included.

KIT D816V-inconclusives

As mentioned earlier, some results were deemed inconclusive due to technical flaws, low abundancy or single-positivity. These samples are marked in the 1D-spectra overview in Appendix 3. Out of the 123 samples that were deemed inconclusive at first, most (n = 66) were re-tested and deemed conclusive subsequently. The remaining 57 samples were either not re-tested, in the case of a single-positive result, or remained technically inferior after re-determination.

Low-abundant samples were characterized by having too few positive droplets for proper conclusion, failing the limit of detection. Furthermore, these droplets were often found at relatively low amplitudes, rendering it harder to differentiate from a dispersed negative signal. Although most samples proved to be negative after re-testing, a subset of 7 samples (16-0108, 16-0950, 17-1802, 19-2753, 20-0422, 20-0762 and 16-1353) was deemed positive upon using 4 wells for the ddPCR assay. When inspecting collection dates of low-abundant samples, most were taken in 2016. The distribution is as follows: 10 samples from 2016, 4 from 2017, 4 from 2018, 3 from 2019 and 5 from 2020.

Arguments for deeming samples technically inferior included no or too few total droplets generated, no or too few WT-positive droplets, major shifts in baseline amplitude or the occurrence of heavy rain. Most (n = 36) technically inferior samples were deemed negative upon re-testing. In total, 4 samples were deemed positive after re-determination, although 2 of these were mainly included for quantification purposes. The remaining 7 samples remain inconclusive. When inspecting collection dates, most samples were taken in 2017. The distribution is as follows: 12 samples from 2016, 17 from 2017, 7 from 2018, 5 from 2019 and 6 from 2020.

Samples were deemed single-positive when only one, or in rare cases 2, positive event was found. Seeing as these samples were not re-tested, they remain inconclusive (n = 50). When inspecting collection dates, most samples were taken in 2019. The distribution is as follows: 7 samples from 2016, 12 from 2017, 10 from 2018, 14 from 2019 and 7 from 2020. An overview of the samples that remain inconclusive is laid out in table 7 below.

Table 7: An overview of KIT-inconclusive samples. Samples were grouped on reason of ambiguity and number of positive events found. 6 samples had 2 positive events, 44 samples had 1 positive event and 7 samples were concluded as technically inadequate.

KIT-inconclusive (n = 57)	2 events	1 event			Technically inadequate
	20-0745	16-0080	17-1925	19-0499	16-0883
	19-2449	16-0738	17-2167	19-1244	16-0581
	19-1948	16-0781	17-2278	19-1496	17-0872
	19-0399	16-1101	18-0163	19-1554	20-1609
	17-2276	16-1400	18-0276	19-1872	18-0071
	20-1417	16-1998	18-0479	19-2464	20-1638
		16-2029	18-1042	19-2853	16-1408
		17-0312	18-1727	20-0043	
		17-0407	18-1752	20-0566	
		17-0574	18-1767	20-1056	
		17-1146	18-2101	20-1165	
		17-1322	18-2718	20-1181	
		17-1483	18-2210	19-1918	
		17-1830	19-0334	19-2346	
		17-1913	19-0347		

As depicted above, most inconclusive samples had one sole positive event (n = 44). Due to the majority of KIT-inconclusive samples not being re-tested (n = 50), and thus lacking any potential consistent factor, further investigation of the characteristics of these samples was futile. Interestingly however, are the samples that remained technically inadequate even after retesting. Most (n =4) of these samples were collected in 2016-2017, in which DNA isolation was less optimal as compared to later years. Furthermore, samples 20-1609 and 18-0071 were tested multiple times and showed low abundancy in more technically adequate measurements. Even apart from the technical inadequacy, these samples therefore would remain inconclusive.

Clinical patient data

In order to find correlation between concomitant presence of KIT D816V in MPN and clinical presentation, patient history of intern UMCG patients was scrutinized. Conclusive diagnoses of patients were scored to accommodate comparison of KIT-positive and KIT-negative patients. Other aspects like the occurrence of multiple mutations were also regarded, based on available NGS data.

Diagnostic Scoring

Diagnoses were investigated and scored on severity of disease. Patient history was reviewed extensively to come to a conclusive diagnosis and therefore a conclusive score. An overview of these patient characteristics can be found in Appendix 2.

In total, 171 patients were included and scored according to table 4. Patients harbouring the KIT D816V mutation (n = 18) were separated from KIT-negative patients (n = 153). A summary of the diagnoses and corresponding frequencies found in each group are shown below in table 8.

Table 8: Distribution of diagnose scores in KIT D816V-positive (n = 18) and KIT-negative (n = 153) patients. Frequency relative to subgroup is shown between parentheses.

Score	KITD816V-Positive	KITD816V-Negative	Diagnose
A	-	-	No SM or MPN conclusively diagnosed
B	-	6 (3,9 %)	SM/MPN suspicion
B(+)	-	1 (0,7 %)	ofPMF&ET suspicion
C	2 (11,1 %)	-	SM
D	1 (5,6 %)	-	SM + MPN suspicion
E	3 (16,7 %)	29 (19,0 %)	ET
F	1 (5,6 %)	22 (14,4 %)	PV
G	-	10 (6,5 %)	PV&ET
H	-	7 (4,6 %)	ET + MF gr 1
I	1 (5,6 %)	4 (2,6 %)	pfPMF (gr 0-1)
J	-	12 (7,8 %)	ofPMF (gr 2-3)
K	-	13 (8,5 %)	Post-PV or Post-ET&PV + MF gr 1
L	2 (11,1 %)	-	SM-MPN
M	2 (11,1 %)	-	SM-MPN + MF gr 2-3
N	-	24 (15,7 %)	Post-PV/ET MF gr 2-3
N (+ L)	1 (5,6 %)	-	Post-PV/ET MF gr 2-3 (+ SM)
N+ (O)	-	1 (0,7 %)	Post-ET MF gr 2-3 + MDS suspicion
O	2 (11,1 %)	9 (5,9 %)	MDS/CML
O (+ L)	1 (5,6 %)	-	MDS/CML + SM
O+ (Q)	-	1 (0,7 %)	CML + AML suspicion
P	-	6 (3,9 %)	MDS/CML + MF gr 2-3
Q	-	4 (2,6 %)	AML
R- (/P)	-	1 (0,7 %)	AML + MDS suspicion
R	2 (11,1 %)	3 (2,0 %)	AML + MF gr 2-3

In KIT D816V-positive patients, most (n = 3, 16,7%) were diagnosed with ET. Further deteriorated diagnoses marked by either presence of MDS, AML, concomitant SM or severe MF progression accounted for a significant part (n = 10, 55,6%) of this subgroup. Patients with generally more indolent diagnoses, such as ET, PV or pfPMF accounted for a relatively small portion (n = 5, 27,8%). Even though all patients included harbored either a JAK2 or CALR mutation, some patients (n = 3, 16,7%) were never conclusively diagnosed with MPN according to available clinical history. This subset was diagnosed with SM instead, one patient was suspected of MPN. In 4 (22,2%) patients SM-MPN was diagnosed, 2 of which with a progression to MF grade 2-3.

Similar to the KIT-positive subgroup, most (n =29, 19,0%) of the KIT-negative patients were diagnosed with ET. In this subgroup, patients with largely indolent diagnoses like ET, PV, MF gr 0-1 or combinations of these accounted for the biggest portion (n= 85, 55,6%). Unlike seen in KIT-positive patients, further deteriorated diagnoses marked by either presence of MDS/CML, AML and/or severe MF progression accounted for a comparatively smaller portion (n = 61, 39,9%). Few patients (n = 7, 4,6%) were only suspected of SM or MPN, one of which was suspected for both ET and PMF.

NGS data

To investigate potential correlations between the occurrence of other mutations beside the aforementioned KIT, JAK, CALR and MPL mutations, available NGS data was analyzed. In Appendix 5 an overview of the collected data can be found. In table 9 below, the summary of characteristics is laid out. Type of diagnose was achieved by using the system laid out in table 4, letters J and L-R were classified as deteriorated.

Table 9: Summary of NGS cohort characteristics of KIT-positive and KIT-negative MPN patients. Listed are the frequencies of number of mutations, type of sample and type of diagnosis. Some patients had both BM and PB samples tested, illustrated by the BM&PB column. Two patients had only a suspected diagnosis and are included within the parentheses.

	No. other mutations	1 mutation	2-3 mutations	4-6 mutations	PB	BM	BM&PB	Indolent diagnoses	Deteriorated diagnoses
KIT-positives (n=5)	1	2	1	1	2	2	1	1	4
KIT-negatives (n=70)	16	22	24	8	30	31	9	36 (38)	32
Total (n=75)	17	24	25	9	32	33	10	37 (39)	36

When observing the number of mutations in this cohort, most patients seem to bear 1 or 2-3 mutations, 24 (32,0%) and 25 (33,3%) respectively. Distribution between type of sample and type of diagnosis did not seem to have bias towards either end. Upon viewing the differences between KIT-Positives and KIT-negatives however, the data suggests a tendency towards more deteriorated diagnoses for KIT-positives. Here, 4 out of 5 diagnoses (80,0%) were deemed deteriorated, as compared to 32 out of 70 (45,7%) diagnoses for KIT-negative patients. Distribution of mutation types has also been inspected from this NGS data, results are visible in table 10 below.

Table 10: Frequency of mutation types in KIT-positive and KIT-negative subgroups, and the total cohort. 'Other' mutations comprised of mutations found in 1 patient. Due to a subset of patients harboring multiple mutations in the same gene, the amount of unique patients harboring the gene in question is shown between parentheses.

	KIT-positives (n=10)	KIT-negatives (n=110)	Total (n=120)
ASXL1	-	23	23 (17)
SRSF2	1	2	3
TET2	3 (2)	32 (26)	35 (28)
TP53	-	12	12 (11)
U2AF1	-	10	10
NRAS	1	2	3
DNMT3A	1	7	8
SF3B1	1	3	4
CBL	-	3	3
SETBP1	-	2	2
EZH2	-	4	4 (3)
IDH2	-	3	3
RUNX1	-	3	3
CSF3R	-	2	2
Other	3	2	5

As evident above, mutations in the TET2 gene were most common in both the total cohort (n = 35, 29,2%) and KIT-negatives (n = 32, 29,1%) with similar ratios. Different mutations in the same gene and patient are included here as well, frequencies with unique gene mutations are shown between parentheses. 'Other' mutations had a frequency of 1 and included mutations in GATA2, KRAS, PTPN11, IKZF1 and IZRSR2. Noteworthy is the frequency of 'other' mutations in the KIT-positive subgroup, comprising of GATA2, KRAS and PTPN11 mutations. Out of 5 patients with 'other' mutations found in the total cohort, 3 were KIT-positive.

A more thorough analysis of NGS data, clinical implications, mutation types and VAF-percentages was attempted. However, due to the relatively small scale of this cohort and thus a low amount of KIT-positive patients, a correlation analysis could not be performed. Moreover, due to the dataset being partially incomplete and limited, patients could not be compared comprehensively.

Discussion

KIT D816V mutation in JAK2/CALR-positive MPN

In a cohort of 321 MPN patients with either the JAK V617F or a CALR mutation, a ddPCR assay on KIT D816V was carried out. Sample results were not exclusively conclusive, but after re-testing most ambiguous samples a decisive choice could be made.

In total, 29 out of 321 patients were concluded to harbor the KIT mutation, resulting in a prevalence of 9,1%. This is significantly higher than previously found in studies. For example, Craig et al found a prevalence of 5,8% of SM in BCR-ABL1-negative MPNs. (29) The KIT D816V mutation is essentially intertwined with SM, both in pathogenesis and diagnosis. KIT mutations are almost invariably (99%) found in SM patients. (30) Samples that were deemed single-positive were not re-tested and therefore did not reach a conclusion. Upon removal of these samples from the cohort, prevalence was higher with 10,7%. Although negating a section of the cohort introduces bias and therefore cannot be interpreted as proof, it does suggest that actual prevalence might be even higher.

Prevalence of KIT-positives within JAK-positive patients was compared with KIT-positive patients harboring a CALR-mutation. A favour towards JAK2-mutations in KIT-positive patients was found, since 93,1% of KIT-positive patients were positive for JAK2 as well. Such a tendency has not yet been described in current research and little is known about the prevalence of KIT combined with either JAK2 or CALR mutations. Further research should be carried out, to potentially elaborate on the relation witnessed here.

KIT D816V-positives

Within the samples of patients deemed KIT D816V-positive, corresponding copies/µl and VAF-percentages were calculated. A strong correlation between KIT allele burden and disease activity/subtype and even overall survival has been found in multiple past studies. (30, 32). Here, patients with advanced SM such as ASM, MCL or SM-AHN showed considerably higher allele burden as compared to ISM. Moreover, patients with higher allele burdens showed strongly increased tryptase levels as well. (30). This train of thought is emphasized by more recent research, in which a higher allele burden was found to correlate with SM progression and overall survival. (48) All in all high allele burdens of KIT D816V in either PB or BM suggest multi-lineage hematopoietic involvement and a more aggressive clinical course of SM.

Samples of low abundance were mostly deemed positive due to consistent finding of positive droplets. Upon comparing BM and PB samples, no real trend was detected. Interestingly, when observing the distribution of single KIT-positive and double positive droplets, samples with lower total amount of KIT-positive droplets showed a higher frequency of single-positives. Perhaps low abundant targets tend to have more single-positive droplets. However, this could also be due to distribution bias, since this finding is relatively scarce in our cohort. From all positive droplets, an average of 2% was found to be single-positive in high abundant targets P1-P7. In the remaining lower abundant targets, samples either showed a highly increased frequency (3 - 25%) of single-positive droplets, or showed no such droplets at all. Little is known about the specific conditions leading to differentiation of single- and double-positive droplets, both in analytical and clinical context.

Inconclusive samples

Within all samples available from patients within our cohort, a substantial number of results proved to be inconclusive at first. Apart from single-positive results, these samples were re-tested to reach a definitive conclusion. General potential reasons for said ambiguity include wrong handling of droplets and reaction mixtures, droplet generation errors or possible degradation of older samples. Furthermore, an overload of either sample DNA or reaction mixture could explain part of the divergent results as well.

Low-abundant

Low abundant samples generally lacked in amount or amplitude of positive droplets. As shortly mentioned earlier, these samples were deemed conclusively positive upon sufficient results in later tests. Patient P8 is the exception, due to only being re-tested for quantification purposes. Apart from this previously deemed positive sample, 6 new patients were deemed as KIT-positive subsequently to retesting.

Noteworthy is the distribution between BM and PB samples of this subgroup, as compared to the total cohort. In all samples tested, 76 out of 369 (20,6%) came from BM material. In this subgroup of low abundant targets however, 10 out 26 (38,5%) samples were collected from BM. This increase may hint towards the belief that results from BM samples could have higher sensitivity.

When regarding the year of sample collection, it becomes evident that most samples included in this subgroup were relatively old. Most samples (n=10, 38,5%) were collected in 2016 and 53,8% of samples were collected between 2016-2017. This frequency substantially exceeds that of other subgroups. The increased frequency could potentially be explained by the suboptimality of the isolation method used in these years, as well as possible degradation of the sample over time.

As seen in sample 16-0108, sample 20-0761 showed a 2D plot that rendered suspicion of aspecific binding. Aspecific binding is a known problem, although reasons and implications are poorly covered in research. In sample 20-0761 aspecific binding seemed to be happening with both probes, illustrated by the severe amplitude increase on both channels. In patient P19 however, aspecific binding seemed to be limited to channel 2 (WT).

Single-Positive

Single-positive samples were generally characterized by the finding of one single-positive droplet, often with a significantly high amplitude. In the scope of this study, all but one have not been retested and their conclusion remains unclear. Little is known about the specific causes and implications of findings like these, provoking this subgroup as a proper future research candidate.

In this subgroup, 8 of 50 (16,0%) samples were collected from BM, which is slightly lower than percentage of total BM samples in this cohort (20,6%). This small decrease holds little significant value and shows no trend.

Generally later samples seem to make up most of this subgroup, as compared to uncertain and technically inferior samples. Most samples were collected in 2019, when the more optimized isolation method was used. The cause of single-positives therefore can hardly be assigned to BM/PB bias, possible degradation of samples or isolation method.

It has not yet been elucidated whether single-positive droplets might be attributed to contamination, a severely low abundancy, or potential other factors. Patients with samples that were deemed single-positive and had other samples available, showed either subsequent negativity or similar single-positivity. It remains unclear whether this is due to post-treatment collection or other factors.

An interesting case within this context is made by results of one patient, in which multiple samples were available: 18-2100, 19-1170 and 20-0745. None of the samples reached the same conclusion, rendering this patient completely ambiguous. Sample 20-0745 was included within the single-positive samples and showed 2 positive events. Sample 18-2100 was deemed low abundant at first with 3 positive events but proved to be negative upon re-determination with 4 wells. Lastly, sample 19-1170 was deemed negative as well. Conflicting findings such as these complicate proper explanation but, accentuate the importance of further research on single-positive results.

Technically inferior

Aberrations in technically inferior samples commonly comprised of baseline-shifts, occurrence of rain, lack of WT-positive droplets, lack of total droplets or significantly low amplitudes. In this subgroup, 2 out of 47 (4,3%) samples were isolated from BM material. This distribution is significantly lower than found in other subgroups and the total cohort (20, 6%). Although the size of this group is limited and therefore hindering correlation analysis, a global trend was witnessed. These findings propose that results from PB samples might be less stable in terms of technical quality, as compared to BM samples.

As seen in the low-abundant subgroup, sample collection dates mostly revolved around earlier years. Most samples in the technically inferior subgroup were isolated in 2017, followed by 2016. Together, the years in which the isolation method was less optimized (2016-2017) make up for 29 out of 47 (61,7%) samples. Again, possible degradation and the isolation method used may be the cause for some of the technical aberrations found here.

Baseline-shifts were found between wells, but within wells as well. A possible explanation for this could be inadequate mixing before droplet generation or the aforementioned degradation of samples. The cause of the discovered occurrence of rain, in which droplets with amplitudes ranging between evident positive and negative droplets are present, is generally unclear. (49) Potential explanations include a delayed PCR onset, partial PCR inhibition and damaged positive or negative droplets. Propositions on improving droplet separation have been made, and include lowering the annealing temperature (49) or prolonging the annealing time. (50)

A lack of WT-positive droplets might be attributed to the accidental usage of too little reaction mixture and thus related to handling or technical errors. A lack of total droplets however, can only be explained by potential technical errors of droplet generation/reading, based on findings illustrated in this study. The finding of significantly lower amplitudes for mutant-channel probes is rarely described in literature. In this stage, only speculations on the subject can be made. A possible explanation could be water condensation within the wells, resulting in smaller droplets and therefore distorting background fluorescence. Condensation may occur more heavily when PCR plates are read immediately after amplification, which has happened numerous times within this study.

Samples that remained inconclusive due to either a lack of re-testing or technical inadequacy showed no significant trend in collection date(s) or sample type (BM/PB). These samples should be included in further research to elucidate potential factors and outcomes of single-positive results and possibly degraded samples.

Clinical patient data

Available patient data was scrutinized on conclusive diagnoses to compare clinical outcomes and progression of KIT-positive and KIT-negative MPN patients. Furthermore, available NGS data was compared to elucidate correlations and distribution of additional mutations within KIT-positive and KIT-negative MPN patients.

Diagnostic scores

A diagnostic scoring table has been set up to differentiate severity of disease within the analyzed cohort. Patients were scored accordingly and distribution in KIT-positive and KIT-negative patients was analyzed and compared. Diagnostic scoring was done with finding a global trend, rather than umabiguous specificiets, in mind. This limited specific comparison, but aided disclosure of general tendencies. Patients with a combination of diagnoses were scored accordingly, slightly increasing the expected severity of disease.

In 10 out of 18 (55,6%) KIT-positive patients, deteriorated diagnoses such as MDS, AML, SM-MPN or severe MF progression (past grade 2) were found. This percentage significantly exceeds the frequency found in KIT-negative patients, in which only 61 of 153 (39,9%) patients had deteriorated diagnoses. It therefore seems that KIT-positive patients indeed are more likely to present more aggressive forms of disease and progression. This concurs with the hypothesis laid out in this study, as well as previous research. (51)

NGS mutation analysis

Although NGS data was limited both in terms of size as well as additional clinical findings, an attempt to find correlations in KIT-positive and KIT-negative patients was made.

Upon comparing diagnoses and average number of mutations in both subgroups, a clear differentiation is detectable. Although difference in number of mutations between subgroups did not prove substantial, a critical difference in deterioration of diagnose was found. In KIT-negative patients 32 out of 70 (45,7%) diagnoses were classified as deteriorated, whereas in KIT-positive patients the prevalence seems to be significantly higher with 4 out of 5 (80,0%) diagnoses deemed severely progressed. Although this cohort is reasonably limited, this data does suggest that KIT-positive patients are more susceptible for aggressive clinical courses and increased progression. Together, findings like these underline our initial hypothesis, confirmed by previous research on correlation between KITD816V and progression. (51)

In KIT-negative patients, most frequent mutations included TET2, ASXL1 and TP53. In KIT-positive patients however, a relatively high frequency of uncommon mutations was found. Mutations in TET2 still proved to be frequent, but the majority of mutations found once in the entire cohort were within the KIT-positive subgroup, despite the limited cohort. Could a KIT-mutation be indicative of these uncommon mutations, or are these mutations perhaps indicative of the KIT D816V mutation. Upon including previous research, it seems that results here are not bordering on discrepancy. In the aforementioned study by Craig et al. (29) a similar occurrence of mutations was found within a KIT-positive cohort. When regarding the MDS-MPN(u) and MPN patients within their cohort, the uncommon mutations KRAS and PTNP11 are found as well, in addition to more common mutations such as TET2, SRSF2 and ASXL1. When compared to combined NGS research in MPNs without a SM-component or KIT D816V mutation, little to no occurrence of either GATA2, PTNP11 or KRAS are found. (52)

An especially compelling case was found in a patient who harbored a JAK2, CALR and MPL mutation simultaneously according to NGS analysis. Patients with co-occurrence are highly scarce and have only recently been described in rare cases. In most studies, no such patients were found and these mutations have therefore been regarded as mutually exclusive. (53, 54) Cases with co-occurrence were limited to a combination of either JAK and MPL mutations or CALR and MPL (55) mutations, but description is made of triple-positive MPN patients. Data on this patient in particular should therefore be scrutinized more extensively in the future.

Future research

In order to find more conclusive correlations, a larger cohort for establishing prevalence of KIT D816V within MPN would be desirable. Moreover, with less ambiguous diagnoses more focus could be laid on discrepancies in overall survival, disease burden and risk/extent of progression. Additionally, retesting of single-positives could elucidate potential causes and implications of these findings, as they remain inconclusive in this study.

For diagnostic scoring, a less limited cohort is even more essential. Elaborate data on these patients could provide for a true correlation analysis, in combination with a more specific grading system than used here. As research develops, a grading system that takes all facets of disease in account could be strategized. Results could prove to be more accurate and valuable when correlations apart from a general trend are evaluated.

Within the NGS analysis, more information and a less limited cohort would be highly beneficial as well. This could facilitate a true comparison of disease burden and specific mutation genes and frequencies.

Lastly, due to sheer rarity, it would be worthwhile to scrutinize available data on the patient with co-occurrence of JAK2, CALR and MPL.

Conclusion

The KIT D816V mutation was detected in 9,1% of MPN patients harboring either JAK2 V617F or CALR mutations. Moreover, upon comparison there seemed to be an inclination towards JAK2 V617F within KIT-positive patients. In JAK2-positive patients 10,6% harbored KIT D816V as well, whereas only 3,0% of CALR patients were deemed KIT-positive. This conception was underlined of the higher prevalence of JAK2 within KIT-positive patients (93,1%), as compared with JAK2 in the total cohort (79,4%). Due to a subset of samples remaining inconclusive, actual prevalence might exceed frequencies found here. Diagnostic scoring of patients suggested a significant impact on disease severity upon co-occurrence of these mutations. Deteriorated diagnoses such as MDS, AML, SM-MPN or severe MF progression were more prevalent in KIT-positive patients (55,6%) in contrast to KIT-negative patients (39,9%). This finding was strengthened by NGS analysis, in which 80% of KIT-positive patients showed deteriorated diagnoses, in comparison with 45,7% in KIT-negative cases. Furthermore, NGS data showed a favour towards less common mutations such as KRAS, PTNP11 and GATA2 in KIT-positives. However, due to scarcity of data and cohort size, NGS analysis could not provide statistically significant evidence. Therefore, future research should expand on this analysis when more data is available. Likewise, more elaborate data and a larger cohort would be beneficial in the KIT D816V-assay and diagnostic scoring. KIT D816V seems to be more prevalent in MPN than previously thought and holds serious clinical implications. Further analysis of inconclusive cases could demonstrate an even higher prevalence than found here.

Bibliography

1. **WHO Classification of Tumours of Haematopoietic and Lymphoid Tissues (4th edition)** Swerdlow, S., Campo, E., Harris, N., Jaffe, E., Pileri, S., Stein, H., & Thiele, J. **(2017)**. *WHO classification of tumours of haematopoietic and lymphoid tissues*. Lyon: International Agency for Research on Cancer.
2. **Grinfeld, J., Nangalia, J., & Green, A. (2016).** Molecular determinants of pathogenesis and clinical phenotype in myeloproliferative neoplasms. *Haematologica*, *102*(1), 7-17. doi: 10.3324/haematol.2014.113845
3. **Mead, A., & Mullally, A. (2017).** Myeloproliferative neoplasm stem cells. *Blood*, *129*(12), 1607-1616. doi: 10.1182/blood-2016-10-696005
4. **Szuber, N., Mudireddy, M., Nicolosi, M., Penna, D., Vallapureddy, R., & Lasho, T. et al. (2019).** 3023 Mayo Clinic Patients With Myeloproliferative Neoplasms: Risk-Stratified Comparison of Survival and Outcomes Data Among Disease Subgroups. *Mayo Clinic Proceedings*, *94*(4), 599-610. doi: 10.1016/j.mayocp.2018.08.022
5. **Tefferi, A., Guglielmelli, P., Larson, D., Finke, C., Wassie, E., & Pieri, L. et al. (2014).** Long-term survival and blast transformation in molecularly annotated essential thrombocythemia, polycythemia vera, and myelofibrosis. *Blood*, *124*(16), 2507-2513. doi: 10.1182/blood-2014-05-579136
6. **Guglielmelli, P., Pacilli, A., Rotunno, G., Rumi, E., Rosti, V., & Delaini, F. et al. (2017).** Presentation and outcome of patients with 2016 WHO diagnosis of prefibrotic and overt primary myelofibrosis. *Blood*, *129*(24), 3227-3236. doi: 10.1182/blood-2017-01-761999
7. **Masarova, L., Bose, P., Daver, N., Pemmaraju, N., Newberry, K., & Manshouri, T. et al. (2017).** Patients with post-essential thrombocythemia and post-polycythemia vera differ from patients with primary myelofibrosis. *Leukemia Research*, *59*, 110-116. doi: 10.1016/j.leukres.2017.06.001
8. **Passamonti, F., Giorgino, T., Mora, B., Guglielmelli, P., Rumi, E., & Maffioli, M. et al. (2017).** A clinical-molecular prognostic model to predict survival in patients with post polycythemia vera and post essential thrombocythemia myelofibrosis. *Leukemia*, *31*(12), 2726-2731. doi: 10.1038/leu.2017.169
9. **Barosi, G., Mesa, R., Thiele, J., Cervantes, F., Campbell, P., & Verstovsek, S. et al. (2007).** Proposed criteria for the diagnosis of post-polycythemia vera and post-essential thrombocythemia myelofibrosis: a consensus statement from the international working group for myelofibrosis research and treatment. *Leukemia*, *22*(2), 437-438. doi: 10.1038/sj.leu.2404914
10. **Schanz, J., Tüchler, H., Solé, F., Mallo, M., Luño, E., & Cervera, J. et al. (2012).** New Comprehensive Cytogenetic Scoring System for Primary Myelodysplastic Syndromes (MDS) and Oligoblastic Acute Myeloid Leukemia After MDS Derived From an International Database Merge. *Journal Of Clinical Oncology*, *30*(8), 820-829. doi: 10.1200/jco.2011.35.6394
11. **Stone, R., Mandrekar, S., Sanford, B., Laumann, K., Geyer, S., & Bloomfield, C. et al. (2017).** Midostaurin plus Chemotherapy for Acute Myeloid Leukemia with aFLT3Mutation. *New England Journal Of Medicine*, *377*(5), 454-464. doi: 10.1056/nejmoa1614359
12. **Estey, E. (2018).** Acute myeloid leukemia: 2019 update on risk-stratification and management. *American Journal Of Hematology*, *93*(10), 1267-1291. doi: 10.1002/ajh.25214
13. **Pardanani, A., Lim, K., Lasho, T., Finke, C., McClure, R., Li, C., & Tefferi, A. (2009).** Prognostically relevant breakdown of 123 patients with systemic mastocytosis associated

with other myeloid malignancies. *Blood*, *114*(18), 3769-3772. doi: 10.1182/blood-2009-05-220145

14. **Bose, P., & Verstovsek, S. (2019).** Updates in the management of polycythemia vera and essential thrombocythemia. *Therapeutic Advances In Hematology*, *10*, 204062071987005. doi: 10.1177/2040620719870052
15. **Finazzi, G., Vannucchi, A., & Barbui, T. (2018).** Prefibrotic myelofibrosis: treatment algorithm 2018. *Blood Cancer Journal*, *8*(11). doi: 10.1038/s41408-018-0142-z
16. **Garcia-Manero, G., Chien, K., & Montalban-Bravo, G. (2020).** Myelodysplastic syndromes: 2021 update on diagnosis, risk stratification and management. *American Journal Of Hematology*, *95*(11), 1399-1420. doi: 10.1002/ajh.25950
17. **Tefferi, A. (2008).** Molecular drug targets in myeloproliferative neoplasms: mutant ABL1, JAK2, MPL, KIT, PDGFRA, PDGFRB and FGFR1. *Journal Of Cellular And Molecular Medicine*, *13*(2), 215-237. doi: 10.1111/j.1582-4934.2008.00559.x
18. **Ciboddo, M., & Mullally, A. (2018).** JAK2 (and other genes) be nimble with MPN diagnosis, prognosis, and therapy. *Hematology*, *2018*(1), 110-117. doi: 10.1182/asheducation-2018.1.110
19. **Pietra, D., Rumi, E., Ferretti, V., Buduo, C., Milanesi, C., & Cavalloni, C. et al. (2015).** Differential clinical effects of different mutation subtypes in CALR-mutant myeloproliferative neoplasms. *Leukemia*, *30*(2), 431-438. doi: 10.1038/leu.2015.277
20. **Rumi, E., Pietra, D., Ferretti, V., Klampfl, T., Harutyunyan, A., & Milosevic, J. et al. (2014).** JAK2 or CALR mutation status defines subtypes of essential thrombocythemia with substantially different clinical course and outcomes. *Blood*, *123*(10), 1544-1551. doi: 10.1182/blood-2013-11-539098
21. **Jia, R., & Kralovics, R. (2019).** Progress in elucidation of molecular pathophysiology of myeloproliferative neoplasms and its application to therapeutic decisions. *International Journal Of Hematology*, *111*(2), 182-191. doi: 10.1007/s12185-019-02778-9
22. **Grinfeld, J., Nangalia, J., Baxter, E., Wedge, D., Angelopoulos, N., & Cantrill, R. et al. (2018).** Classification and Personalized Prognosis in Myeloproliferative Neoplasms. *New England Journal Of Medicine*, *379*(15), 1416-1430. doi: 10.1056/nejmoa1716614
23. **Diep, R., & Metjian, A. (2018).** A rare CALR variant mutation and a review of CALR in essential thrombocythemia. *Journal Of Thrombosis And Thrombolysis*, *45*(3), 457-462. doi: 10.1007/s11239-018-1619-0
24. **Nangalia, J., Massie, C., Baxter, E., Nice, F., Gundem, G., & Wedge, D. et al. (2013).** Somatic CALR Mutations in Myeloproliferative Neoplasms with Nonmutated JAK2. *New England Journal Of Medicine*, *369*(25), 2391-2405. doi: 10.1056/nejmoa1312542
25. **Szuber, N., Hanson, C., Lasho, T., Finke, C., Ketterling, R., & Pardanani, A. et al. (2018).** MPL-mutated essential thrombocythemia: a morphologic reappraisal. *Blood Cancer Journal*, *8*(12). doi: 10.1038/s41408-018-0159-3
26. **Rumi, E., Pietra, D., Pascutto, C., Guglielmelli, P., Martínez-Trillos, A., & Casetti, I. et al. (2014).** Clinical effect of driver mutations of JAK2, CALR, or MPL in primary myelofibrosis. *Blood*, *124*(7), 1062-1069. doi: 10.1182/blood-2014-05-578435
27. **Shammo, J., & Stein, B. (2016).** Mutations in MPNs: prognostic implications, window to biology, and impact on treatment decisions. *Hematology*, *2016*(1), 552-560. doi: 10.1182/asheducation-2016.1.552

28. **Tefferi, A., & Pardanani, A. (2018).** Mutations and prognosis in myeloproliferative neoplasms. *Leukemia & Lymphoma*, *60*(5), 1112-1113. doi: 10.1080/10428194.2018.1537490
29. **Craig, J., Hasserjian, R., Kim, A., Aster, J., Pinkus, G., & Hornick, J. et al. (2020).** Detection of the KITD816V mutation in myelodysplastic and/or myeloproliferative neoplasms and acute myeloid leukemia with myelodysplasia-related changes predicts concurrent systemic mastocytosis. *Modern Pathology*, *33*(6), 1135-1145. doi: 10.1038/s41379-019-0447-x
30. **Erben, P., Schwaab, J., Metzgeroth, G., Horny, H., Jawhar, M., & Sotlar, K. et al. (2013)**. The KIT D816V expressed allele burden for diagnosis and disease monitoring of systemic mastocytosis. *Annals Of Hematology*, *93*(1), 81-88. doi: 10.1007/s00277-013-1964-1
31. **Schwaab, J., Schnittger, S., Sotlar, K., Walz, C., Fabarius, A., & Pfirrmann, M. et al. (2013).** Comprehensive mutational profiling in advanced systemic mastocytosis. *Blood*, *122*(14), 2460-2466. doi: 10.1182/blood-2013-04-496448
32. **Hoermann, G., Gleixner, K., Dinu, G., Kundi, M., Greiner, G., & Wimazal, F. et al. (2014).** TheKITD816V allele burden predicts survival in patients with mastocytosis and correlates with the WHO type of the disease. Allergy, 69(6), 810-813. doi: 10.1111/all.12409
33. **Mai, B., Wahed, M., Chen, L., Nguyen, N., Wang, X., & Hu, Z. (2020)**. Educational Case: Systemic Mastocytosis with an Associated Hematological Neoplasm. *Academic Pathology*, *7*, 237428952090652. doi: 10.1177/2374289520906526
34. **Ustun, C., Arock, M., Kluin-Nelemans, H., Reiter, A., Sperr, W., & George, T. et al. (2016)**. Advanced systemic mastocytosis: from molecular and genetic progress to clinical practice. *Haematologica*, *101*(10), 1133-1143. doi: 10.3324/haematol.2016.146563
35. **Pardanani, A. (2018)**. Systemic mastocytosis in adults: 2019 update on diagnosis, risk stratification and management. *American Journal Of Hematology*. doi: 10.1002/ajh.25371
36. **Coltoff, A., & Mascarenhas, J. (2019)**. Relevant updates in systemic mastocytosis. *Leukemia Research*, *81*, 10-18. doi: 10.1016/j.leukres.2019.04.001
37. **Tefferi, A., Shah, S., Lasho, T., Patnaik, M., Reichard, K., & Hanson, C. et al. (2018)**. Practice-relevant demarcation of systemic mastocytosis associated with another hematologic neoplasm. *American Journal Of Hematology*, *93*(12), E383-E386. doi: 10.1002/ajh.25269
38. **Sotlar, K., Bache, A., Stellmacher, F., Bültmann, B., Valent, P., & Horny, H. (2008).** Systemic Mastocytosis Associated with Chronic Idiopathic Myelofibrosis. *The Journal Of Molecular Diagnostics*, *10*(1), 58-66. doi: 10.2353/jmoldx.2008.070061
39. **Sharma, S., Hahn-Ellis, J., Metcalfe, D., & Maric, I. (2017).** Occurrence of JAK2 and CALR Mutations in Patients with Systemic Mastocytosis and Thrombocytosis. *Clinical Lymphoma Myeloma And Leukemia*, *17*, S351-S352. doi: 10.1016/j.clml.2017.07.178
40. **Broesby-Olsen, S., Kristensen, T., Møller, M., Bindslev-Jensen, C., & Vestergaard, H. (2012).** Adult-onset systemic mastocytosis in monozygotic twins with KIT D816V and JAK2 V617F mutations. *Journal Of Allergy And Clinical Immunology*, *130*(3), 806-808. doi: 10.1016/j.jaci.2012.04.013
41. **Koppikar, P., & Levine, R. (2008)**. JAK2 and MPL Mutations in Myeloproliferative Neoplasms. *Acta Haematologica*, *119*(4), 218-225. doi: 10.1159/000140634
42. **Mughal, T., Pemmaraju, N., Radich, J., Deininger, M., Kucine, N., & Kiladjian, J. et al. (2019).** Emerging translational science discoveries, clonal approaches, and treatment trends in chronic myeloproliferative neoplasms. *Hematological Oncology*, *37*(3), 240-252. doi: 10.1002/hon.2622

43. **Taylor, S., Laperriere, G., & Germain, H. (2017).** Droplet Digital PCR versus qPCR for gene expression analysis with low abundant targets: from variable nonsense to publication quality data. *Scientific Reports*, *7*(1). doi: 10.1038/s41598-017-02217-x
44. **Hindson, C., Chevillet, J., Briggs, H., Gallichotte, E., Ruf, I., & Hindson, B. et al. (2013).** Absolute quantification by droplet digital PCR versus analog real-time PCR. *Nature Methods*, *10*(10), 1003-1005. doi: 10.1038/nmeth.2633
45. **Waterhouse, M., Follo, M., Pfeifer, D., von Bubnoff, N., Duyster, J., Bertz, H., & Finke, J. (2016).** Sensitive and accurate quantification of JAK2 V617F mutation in chronic myeloproliferative neoplasms by droplet digital PCR. *Annals Of Hematology*, *95*(5), 739-744. doi: 10.1007/s00277-016-2623-0
46. **Mimiola, E., Bomben, R., De Matteis, G., Perbellini, O., Guglielmelli, P., & Bonifacio, M. et al. (2019).** Systemic mastocytosis associated with myelodysplastic/myeloproliferative neoplasms with ring sideroblasts and thrombocytosis: Report of three cases. *Hematological Oncology*, *37*(5), 628-633. doi: 10.1002/hon.2680
47. **Thachil, J., Hawkins, S., & Woodcock, B. (2011).** JAK2-positive myeloproliferative neoplasm co-existing with systemic mastocytosis. *British Journal Of Haematology*, *152*(6), 675-675. doi: 10.1111/j.1365-2141.2010.08536.x
48. **Greiner, G., Gurbisz, M., Ratzinger, F., Witzeneder, N., Class, S., & Eisenwort, G. et al. (2019).** Molecular quantification of tissue disease burden is a new biomarker and independent predictor of survival in mastocytosis. *Haematologica*, *105*(2), 366-374. doi: 10.3324/haematol.2019.217950
49. **Gerdes, L., Iwobi, A., Busch, U., & Pecoraro, S. (2016).** Optimization of digital droplet polymerase chain reaction for quantification of genetically modified organisms. *Biomolecular Detection And Quantification*, *7*, 9-20. doi: 10.1016/j.bdq.2015.12.003
50. **Witte, A., Mester, P., Fister, S., Witte, M., Schoder, D., & Rossmanith, P. (2016)**. A Systematic Investigation of Parameters Influencing Droplet Rain in the Listeria monocytogenes prfA Assay - Reduction of Ambiguous Results in ddPCR. *PLOS ONE*, *11*(12), e0168179. doi: 10.1371/journal.pone.0168179
51. **Jawhar, M., Schwaab, J., Naumann, N., Metzgeroth, G., Horny, H., & Sotlar, K. et al. (2018).** A New Prognostic Score for Advanced Systemic Mastocytosis Based on Clinical and Genetic Characteristics of 210 Consecutive Patients. *Blood*, *132*(Supplement 1), 349-349. doi: 10.1182/blood-2018-99-115804
52. **Skov, V. (2020).** Next Generation Sequencing in MPNs. Lessons from the Past and Prospects for Use as Predictors of Prognosis and Treatment Responses. *Cancers*, *12*(8), 2194. doi: 10.3390/cancers12082194
53. **Li, M. Y., Chao, H. Y., Sun, A. N., Qiu, H. Y., Jin, Z. M., Tang, X. W., Han, Y., Fu, C. C., Chen, S. N., & Wu, D. P. (2017).** Clinical significance of JAK2,CALR and MPL gene mutations in 1 648 Philadelphia chromosome negative myeloproliferative neoplasms patients from a single center. *Zhonghua xueyexue zazhi, 38(4), 295–300.* doi: 10.3760/cma.j.issn.0253-2727.2017.04.007
54. **Kim, S., Im, K., Park, S., Kwon, J., Kim, J., & Lee, D. (2015).** CALR, JAK2, and MPL Mutation Profiles in Patients With Four Different Subtypes of Myeloproliferative Neoplasms. *American Journal Of Clinical Pathology*, *143*(5), 635-644. doi: 10.1309/ajcpuaac16liwzmm
55. **Kelkar, K., Ramanan, V., Anand, S., Ranade, S., Patil, K., Agarwal, M., & Phadke, N. (2019).** Co-occurrence of CALR and MPL somatic mutations in an Indian patient with a Philadelphia-

negative myeloproliferative neoplasm. *Journal Of Hematopathology*, *12*(3), 163-168. doi: 10.1007/s12308-019-00359-7

Appendix

Appendix 1: Patient characteristics and sample data

Appendix 1 is included within the supplementary data: *Appendix 1. Main table with patient characteristics and sample data.xlsx*

Appendix 2: Diagnostic scoring of intern patients

Appendix 2 is included within the supplementary data: *Appendix 2. Diagnosis scoring and clinical course of intern patients.xlsx*

Appendix 3: ddPCR 1D spectra of all samples

Appendix 3 is included within the supplementary data: *Appendix 3. ddPCR 1D spectra of all samples.xlsx*

Appendix 4: ddPCR 2D spectra of KIT-positive patients

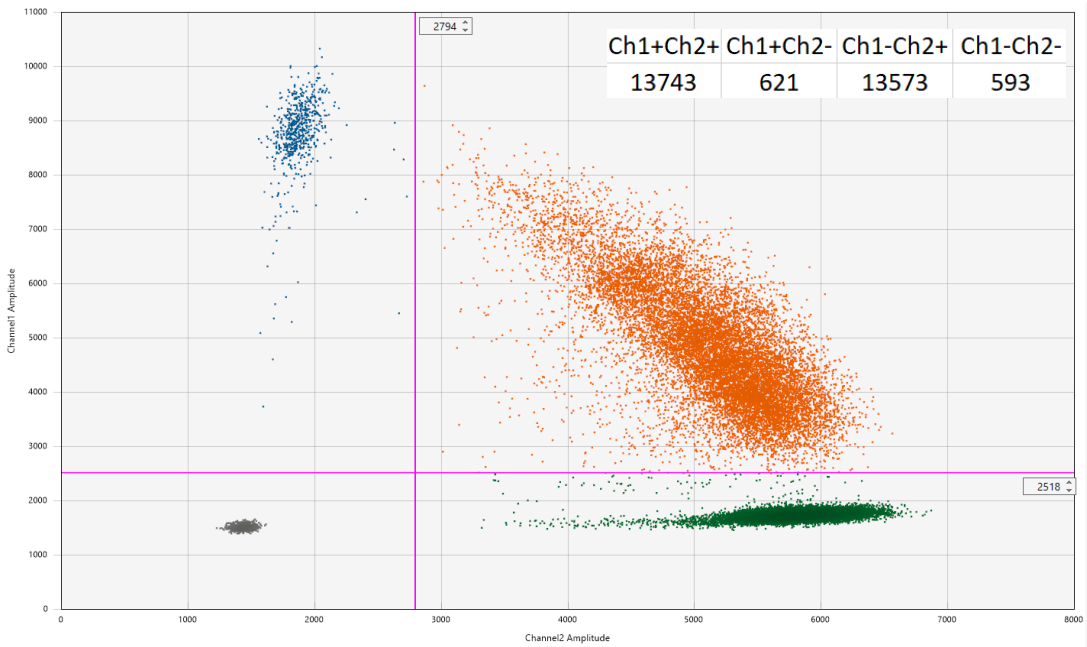

Figure 3: 2D graph of patient P1, with channel 1 amplitude (mutant) on the y-axis and channel 2 amplitude (WT) on the x-axis. Y-axis (2794) and X-axis (2518) thresholds are shown next to the corresponding line. Single KIT-positive droplets are marked by blue droplets. The orange droplets show droplets positive for both channels. Green droplets represent droplets that are solely positive for WT, and grey droplets depict double negative droplets. The number of droplets within each group is shown as well.

In figure 3, the 2D spectrum of patient P1 is shown. With 2 wells combined, 13743 droplets were found to be double-positive. Out of the single-positive droplets, 621 were positive for KIT D816V and 593 for WT. Of all KIT-positive droplets, 4,32% was single-positive.

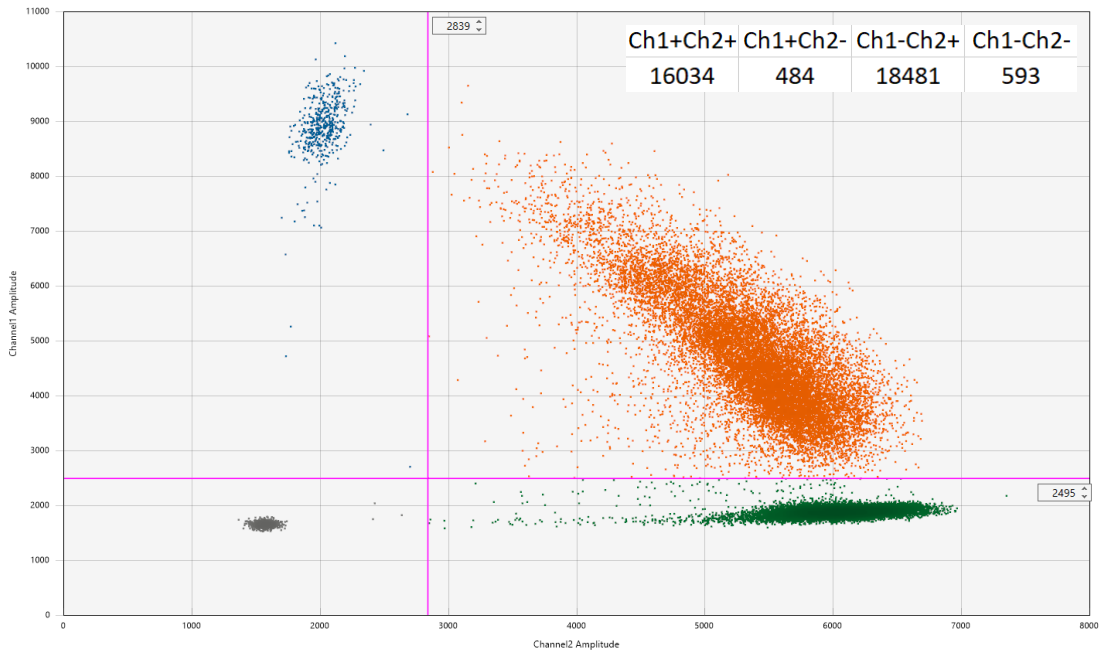

Figure 4: 2D graph of patient P2, with channel 1 amplitude (mutant) on the y-axis and channel 2 amplitude (WT) on the x-axis. Y-axis (2839) and X-axis (2495) thresholds are shown next to the corresponding line. Single KIT-positive droplets are marked by blue droplets. The orange droplets show droplets positive for both channels. Green droplets represent droplets that are solely positive for WT, and grey droplets depict double negative droplets. The number of droplets within each group is shown as well.

In figure 4, the 2D spectrum of patient P2 is shown. With 2 wells combined, 16034 droplets were found to be double-positive. Out of the single-positive droplets, 484 were positive for KIT D816V and 18481 for WT. Of all KIT-positive droplets, 2,93% was single-positive.

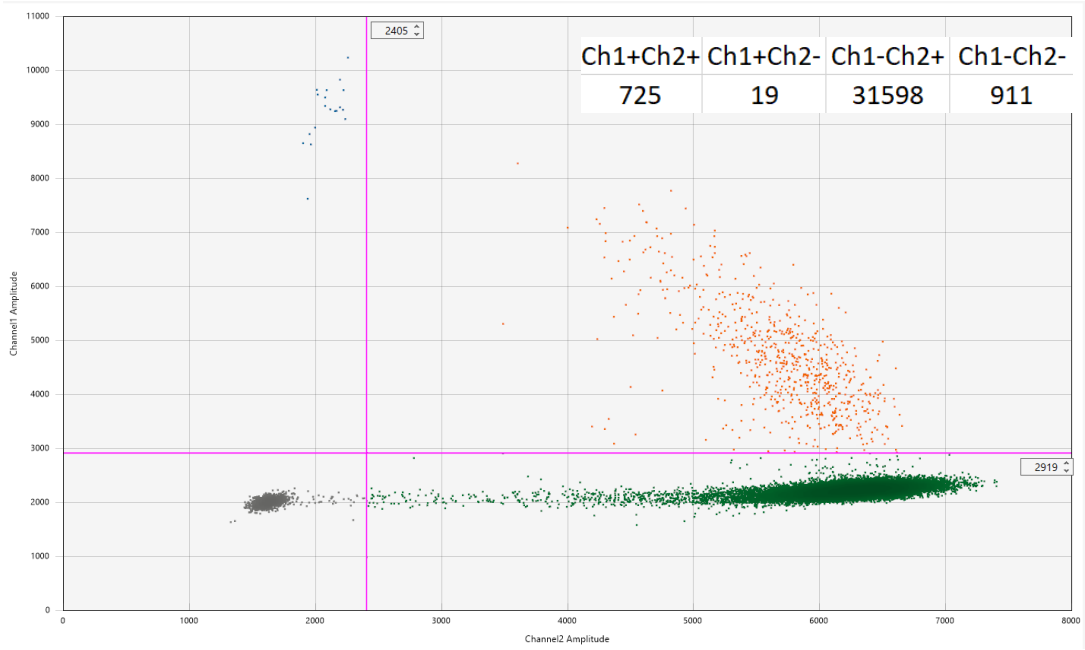

Figure 5: 2D graph of patient P3, with channel 1 amplitude (mutant) on the y-axis and channel 2 amplitude (WT) on the x-axis. Y-axis (2405) and X-axis (2919) thresholds are shown next to the corresponding line. Single KIT-positive droplets are marked by blue droplets. The orange droplets show droplets positive for both channels. Green droplets represent droplets that are solely positive for WT, and grey droplets depict double negative droplets. The number of droplets within each group is shown as well.

In figure 5, the 2D spectrum of patient P3 is shown. With 4 wells combined, 725 droplets were found to be double-positive. Out of the single-positive droplets, 19 were positive for KIT D816V and 31598 for WT. Of all KIT-positive droplets, 2,55% was single-positive.

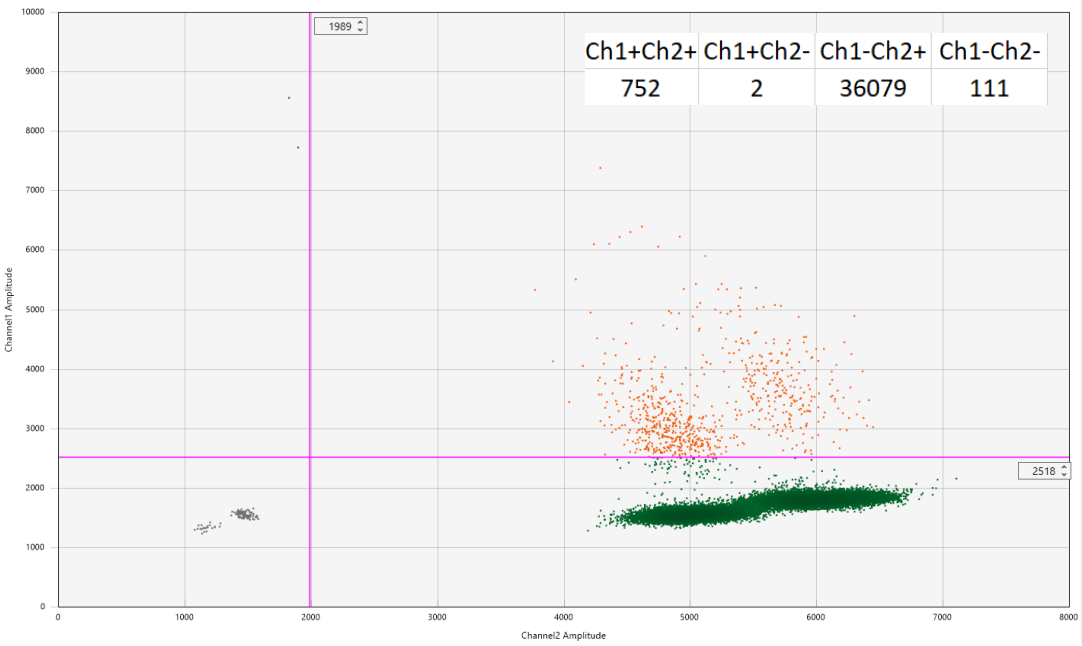

Figure 6: 2D graph of patient P4, with channel 1 amplitude (mutant) on the y-axis and channel 2 amplitude (WT) on the x-axis. Y-axis (1989) and X-axis (2518) thresholds are shown next to the corresponding line. Single KIT-positive droplets are marked by blue droplets. The orange droplets show droplets positive for both channels. Green droplets represent droplets that are solely positive for WT, and grey droplets depict double negative droplets. The number of droplets within each group is shown as well.

In figure 6, the 2D spectrum of patient P4 is shown. With 2 wells combined, 752 droplets were found to be double-positive. Out of the single-positive droplets, 2 were positive for KIT D816V and 36079 for WT. Of all KIT-positive droplets, 0,27% was single-positive.

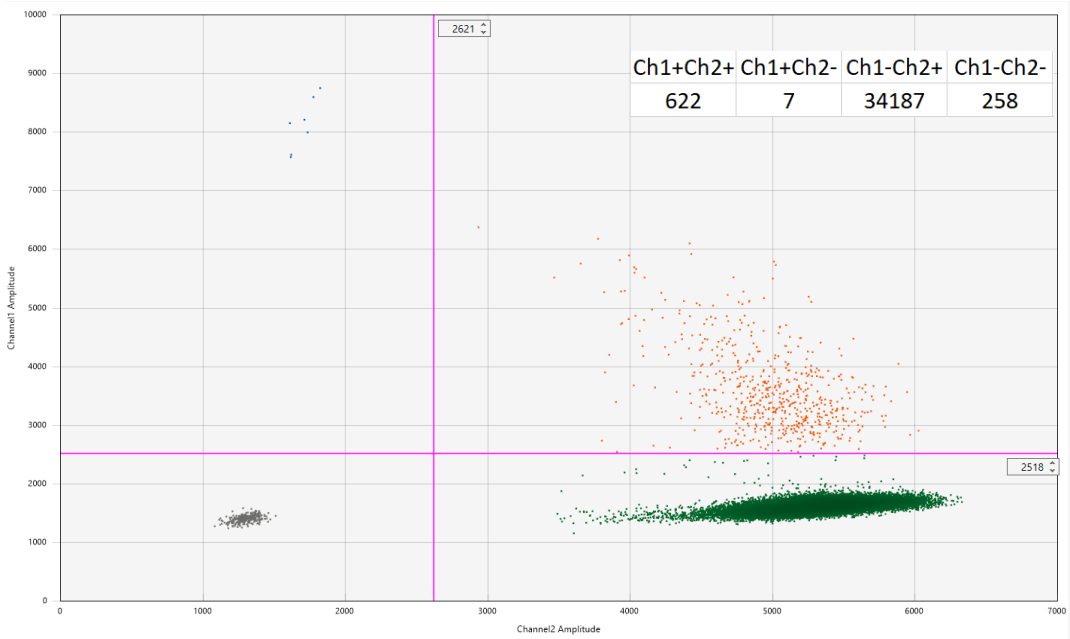

Figure 7: 2D graph of patient P5, with channel 1 amplitude (mutant) on the y-axis and channel 2 amplitude (WT) on the x-axis. Y-axis (2621) and X-axis (2518) thresholds are shown next to the corresponding line. Single KIT-positive droplets are marked by blue droplets. The orange droplets show droplets positive for both channels. Green droplets represent droplets that are solely positive for WT, and grey droplets depict double negative droplets. The number of droplets within each group is shown as well.

In figure 7, the 2D spectrum of patient P5 is shown. With 2 wells combined, 622 droplets were found to be double-positive. Out of the single-positive droplets, 7 were positive for KIT D816V and 34187 for WT. Of all KIT-positive droplets, 1,11% was single-positive.

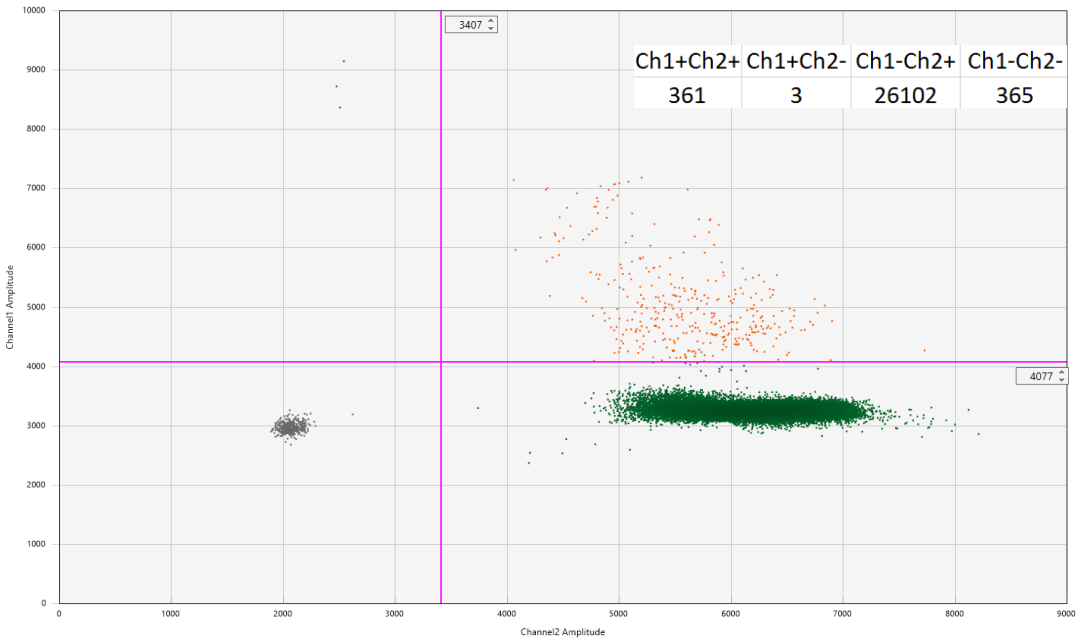

Figure 8: 2D graph of patient P6, with channel 1 amplitude (mutant) on the y-axis and channel 2 amplitude (WT) on the x-axis. Y-axis (3407) and X-axis (3077) thresholds are shown next to the corresponding line. Single KIT-positive droplets are marked by blue droplets. The orange droplets show droplets positive for both channels. Green droplets represent droplets that are solely positive for WT, and grey droplets depict double negative droplets. The number of droplets within each group is shown as well.

In figure 8, the 2D spectrum of patient P6 is shown. With 2 wells combined, 361 droplets were found to be double-positive. Out of the single-positive droplets, 3 were positive for KIT D816V and 26102 for WT. Of all KIT-positive droplets, 0,82% was single-positive.

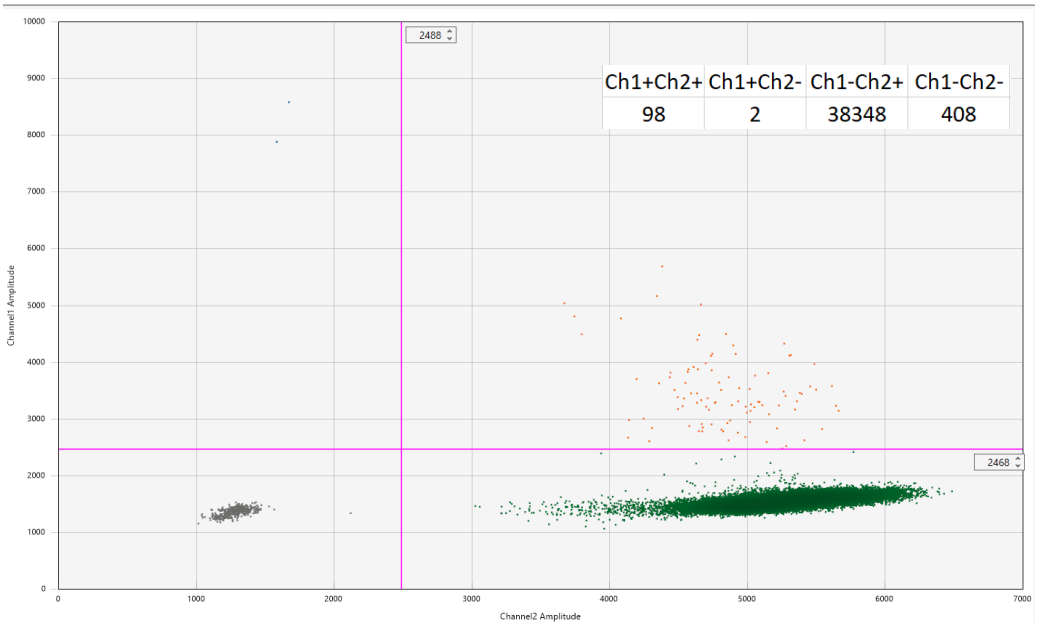

Figure 9: 2D graph of patient P7, with channel 1 amplitude (mutant) on the y-axis and channel 2 amplitude (WT) on the x-axis. Y-axis (2488) and X-axis (2468) thresholds are shown next to the corresponding line. Single KIT-positive droplets are marked by blue droplets. The orange droplets show droplets positive for both channels. Green droplets represent droplets that are solely positive for WT, and grey droplets depict double negative droplets. The number of droplets within each group is shown as well.

In figure 9, the 2D spectrum of patient P7 is shown. With 2 wells combined, 98 droplets were found to be double-positive. Out of the single-positive droplets, 2 were positive for KIT D816V and 38348 for WT. Of all KIT-positive droplets, 2,00% was single-positive.

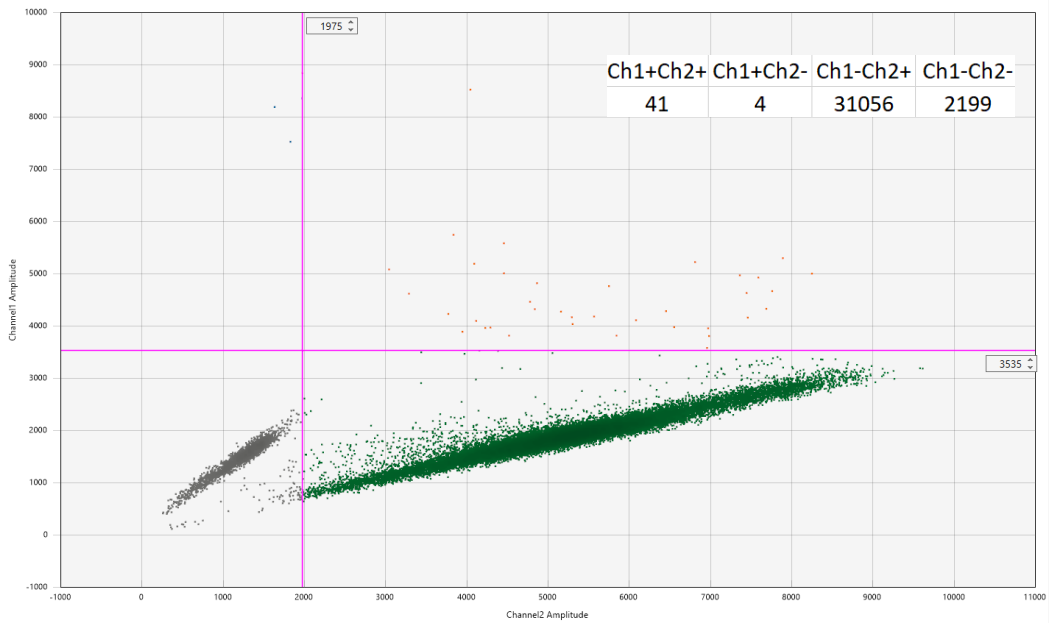

Figure 10: 2D graph of patient P8, with channel 1 amplitude (mutant) on the y-axis and channel 2 amplitude (WT) on the x-axis. Y-axis (1975) and X-axis (3535) thresholds are shown next to the corresponding line. Single KIT-positive droplets are marked by blue droplets. The orange droplets show droplets positive for both channels. Green droplets represent droplets that are solely positive for WT, and grey droplets depict double negative droplets. The number of droplets within each group is shown as well.

In figure 10, the 2D spectrum of patient P8 is shown. With 4 wells combined, 41 droplets were found to be double-positive. Out of the single-positive droplets, 4 were positive for KIT D816V and 31056 for WT. Of all KIT-positive droplets, 8,89% was single-positive.

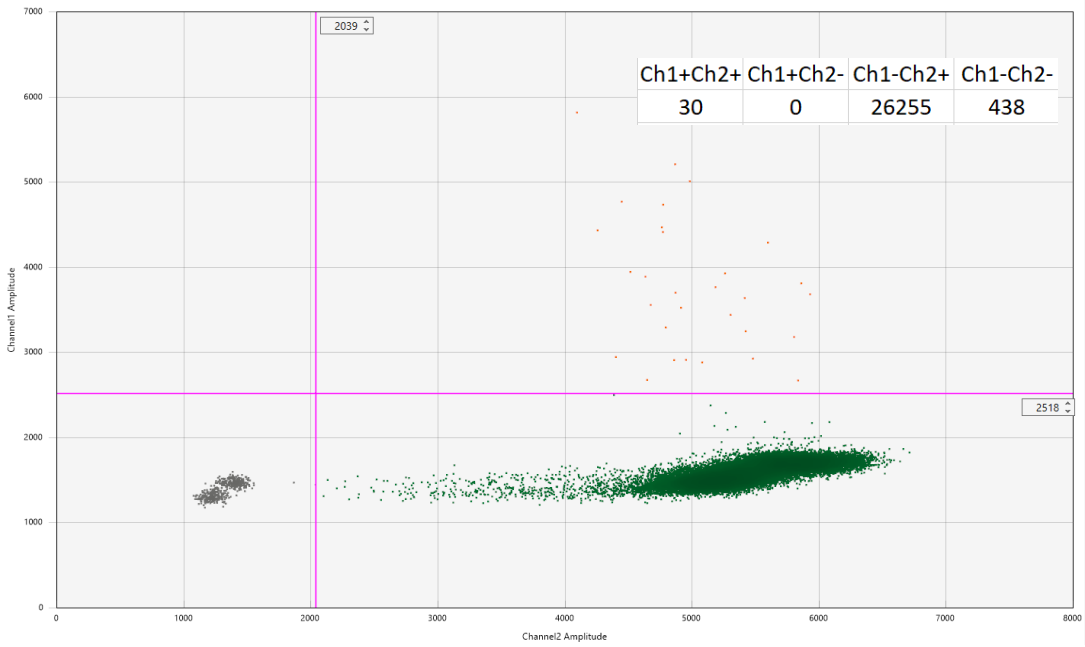

Figure 11: 2D graph of patient P9, with channel 1 amplitude (mutant) on the y-axis and channel 2 amplitude (WT) on the x-axis. Y-axis (2039) and X-axis (2518) thresholds are shown next to the corresponding line. Single KIT-positive droplets are marked by blue droplets. The orange droplets show droplets positive for both channels. Green droplets represent droplets that are solely positive for WT, and grey droplets depict double negative droplets. The number of droplets within each group is shown as well.

In figure 11, the 2D spectrum of patient P9 is shown. With 2 wells combined, 30 droplets were found to be double-positive. Out of the single-positive droplets, 0 were positive for KIT D816V and 26255 for WT.

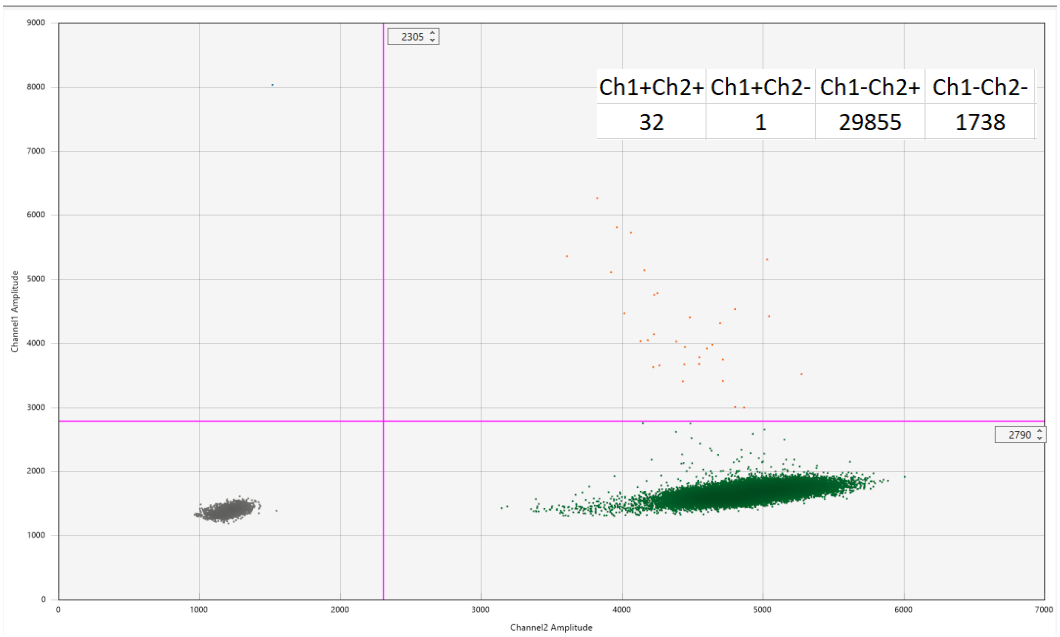

Figure 12: 2D graph of patient P10, with channel 1 amplitude (mutant) on the y-axis and channel 2 amplitude (WT) on the x-axis. Y-axis (2305) and X-axis (2790) thresholds are shown next to the corresponding line. Single KIT-positive droplets are marked by blue droplets. The orange droplets show droplets positive for both channels. Green droplets represent droplets that are solely positive for WT, and grey droplets depict double negative droplets. The number of droplets within each group is shown as well.

In figure 12, the 2D spectrum of patient P10 is shown. With 2 wells combined, 32 droplets were found to be double-positive. Out of the single-positive droplets, 1 was positive for KIT D816V and 29855 were positive for WT. Of all KIT-positive droplets, 3,03% was single-positive.

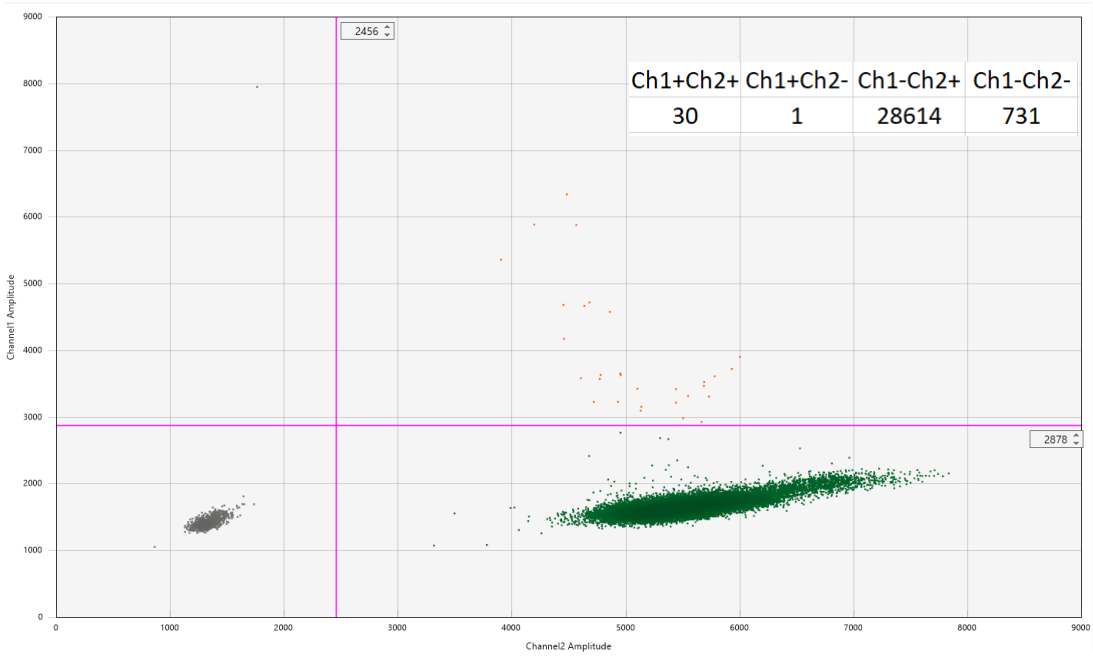

Figure 13: 2D graph of patient P11, with channel 1 amplitude (mutant) on the y-axis and channel 2 amplitude (WT) on the x-axis. Y-axis (2456) and X-axis (2878) thresholds are shown next to the corresponding line. Single KIT-positive droplets are marked by blue droplets. The orange droplets show droplets positive for both channels. Green droplets represent droplets that are solely positive for WT, and grey droplets depict double negative droplets. The number of droplets within each group is shown as well.

In figure 13, the 2D spectrum of patient P11 is shown. With 2 wells combined, 30 droplets were found to be double-positive. Out of the single-positive droplets, 1 was positive for KIT D816V and 28614 were positive for WT. Of all KIT-positive droplets, 3,23% was single-positive.

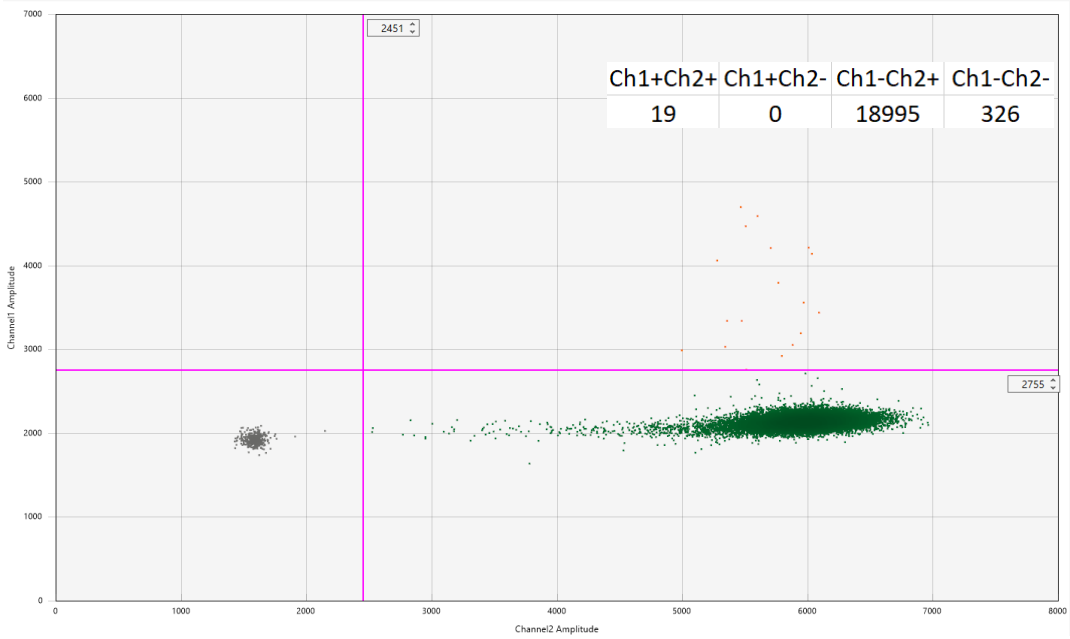

Figure 14: 2D graph of patient P12, with channel 1 amplitude (mutant) on the y-axis and channel 2 amplitude (WT) on the x-axis. Y-axis (2451) and X-axis (2755) thresholds are shown next to the corresponding line. Single KIT-positive droplets are marked by blue droplets. The orange droplets show droplets positive for both channels. Green droplets represent droplets that are solely positive for WT, and grey droplets depict double negative droplets. The number of droplets within each group is shown as well.

In figure 14, the 2D spectrum of patient P12 is shown. With 2 wells combined, 19 droplets were found to be double-positive. Out of the single-positive droplets, 0 were positive for KIT D816V and 18995 for WT.

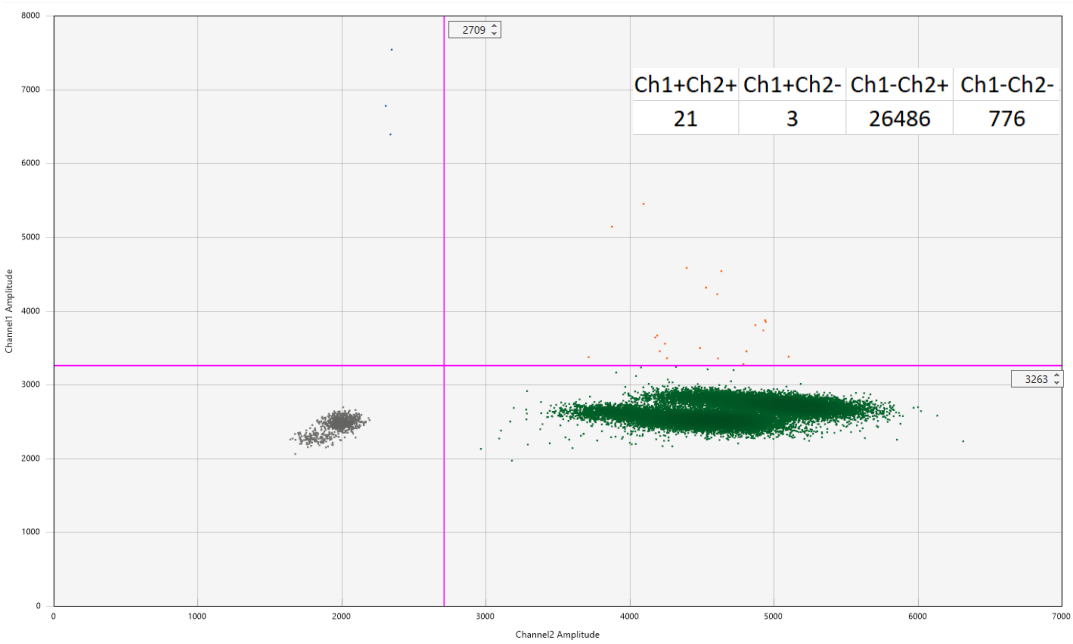

Figure 15: 2D graph of patient P13, with channel 1 amplitude (mutant) on the y-axis and channel 2 amplitude (WT) on the x-axis. Y-axis (2709) and X-axis (3263) thresholds are shown next to the corresponding line. Single KIT-positive droplets are marked by blue droplets. The orange droplets show droplets positive for both channels. Green droplets represent droplets that are solely positive for WT, and grey droplets depict double negative droplets. The number of droplets within each group is shown as well.

In figure 15, the 2D spectrum of patient P13 is shown. With 2 wells combined, 21 droplets were found to be double-positive. Out of the single-positive droplets, 3 were positive for KIT D816V and 26486 for WT. Of all KIT-positive droplets, 12,50% was single-positive.

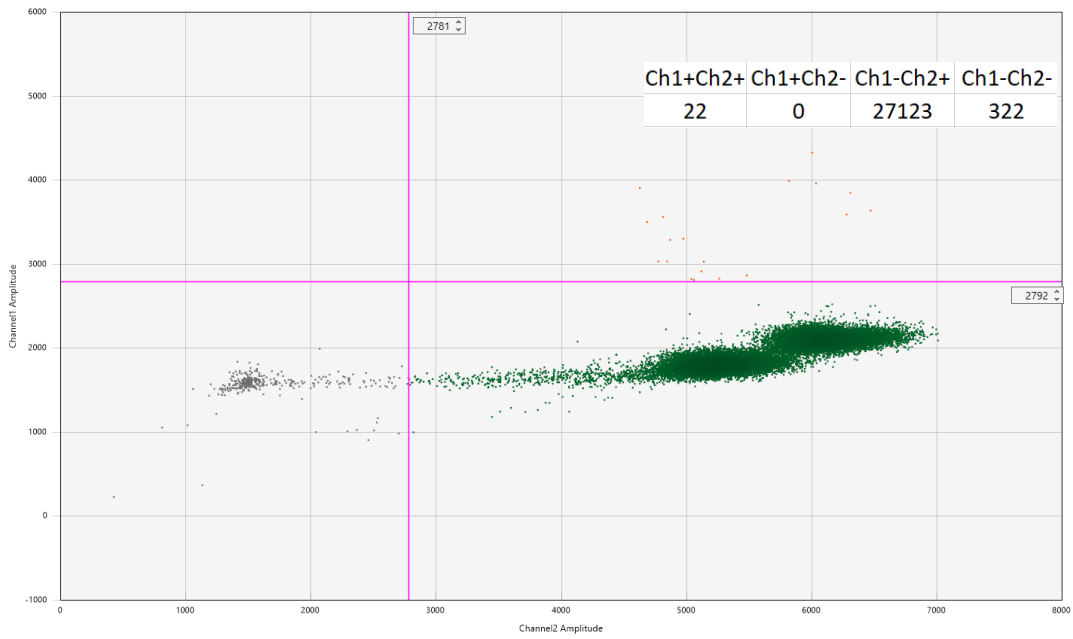

Figure 16: 2D graph of patient P14, with channel 1 amplitude (mutant) on the y-axis and channel 2 amplitude (WT) on the x-axis. Y-axis (2781) and X-axis (2792) thresholds are shown next to the corresponding line. Single KIT-positive droplets are marked by blue droplets. The orange droplets show droplets positive for both channels. Green droplets represent droplets that are solely positive for WT, and grey droplets depict double negative droplets. The number of droplets within each group is shown as well.

In figure 16, the 2D spectrum of patient P14 is shown. With 2 wells combined, 22 droplets were found to be double-positive. Out of the single-positive droplets, 0 were positive for KIT D816V and 27123 for WT.

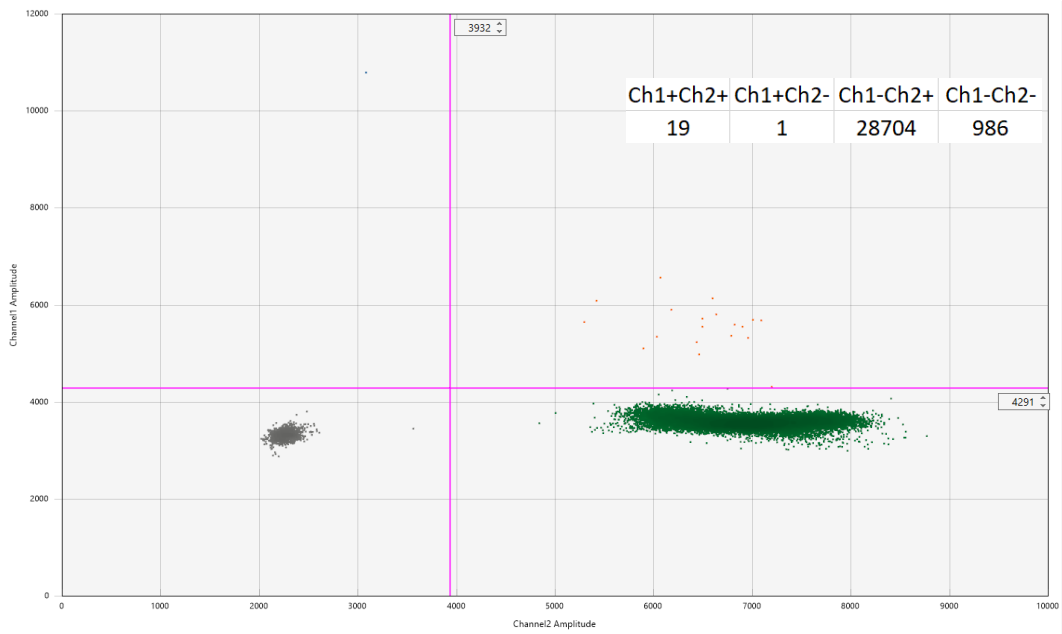

Figure 17: 2D graph of patient P15, with channel 1 amplitude (mutant) on the y-axis and channel 2 amplitude (WT) on the x-axis. Y-axis (3932) and X-axis (4291) thresholds are shown next to the corresponding line. Single KIT-positive droplets are marked by blue droplets. The orange droplets show droplets positive for both channels. Green droplets represent droplets that are solely positive for WT, and grey droplets depict double negative droplets. The number of droplets within each group is shown as well.

In figure 17, the 2D spectrum of patient P15 is shown. With 2 wells combined, 19 droplets were found to be double-positive. Out of the single-positive droplets, 1 was positive for KIT D816V and 28704 were positive for WT. Of all KIT-positive droplets, 5,0% was single-positive.

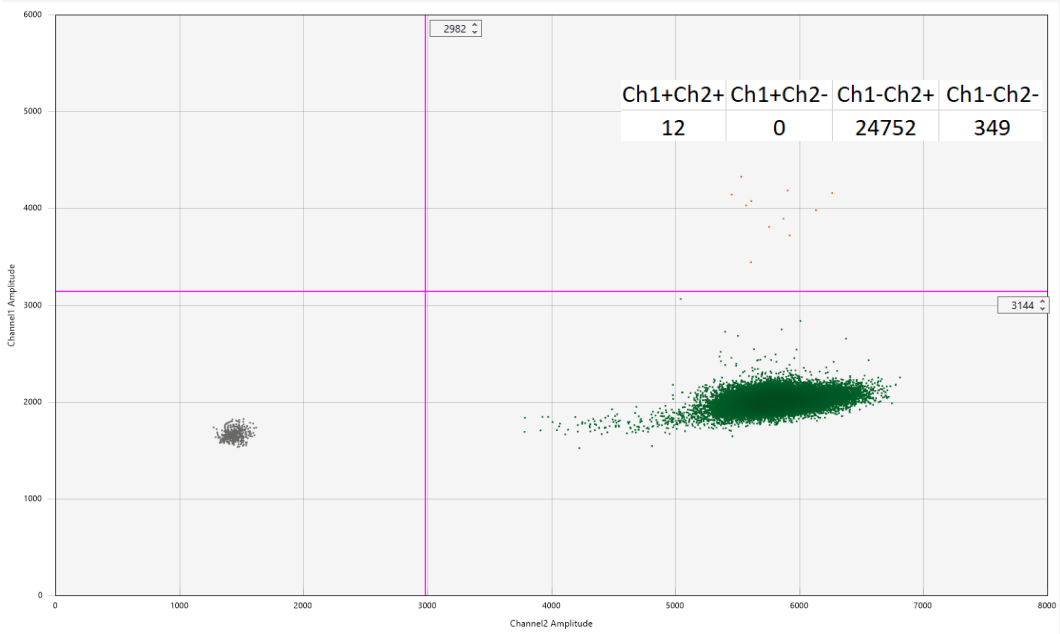

Figure 18: 2D graph of patient P16, with channel 1 amplitude (mutant) on the y-axis and channel 2 amplitude (WT) on the x-axis. Y-axis (2982) and X-axis (3144) thresholds are shown next to the corresponding line. Single KIT-positive droplets are marked by blue droplets. The orange droplets show droplets positive for both channels. Green droplets represent droplets that are solely positive for WT, and grey droplets depict double negative droplets. The number of droplets within each group is shown as well.

In figure 18, the 2D spectrum of patient P16 is shown. With 2 wells combined, 12 droplets were found to be double-positive. Out of the single-positive droplets, 0 were positive for KIT D816V and 24752 for WT.

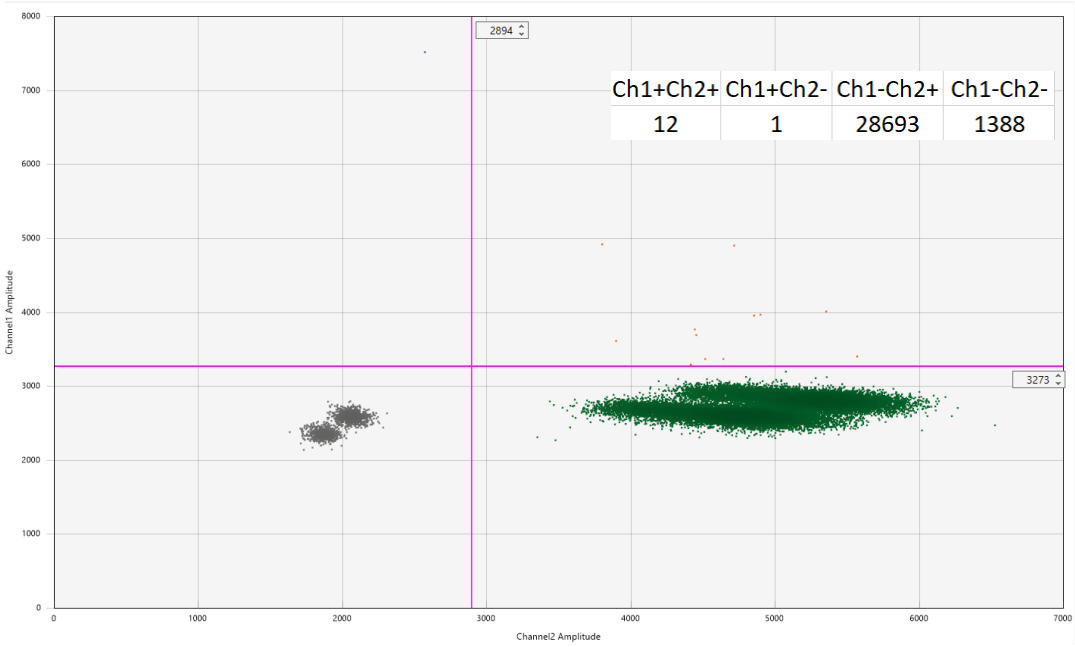

Figure 19: 2D graph of patient P17, with channel 1 amplitude (mutant) on the y-axis and channel 2 amplitude (WT) on the x-axis. Y-axis (2894) and X-axis (3273) thresholds are shown next to the corresponding line. Single KIT-positive droplets are marked by blue droplets. The orange droplets show droplets positive for both channels. Green droplets represent droplets that are solely positive for WT, and grey droplets depict double negative droplets. The number of droplets within each group is shown as well.

In figure 19, the 2D spectrum of patient P17 is shown. With 2 wells combined, 12 droplets were found to be double-positive. Out of the single-positive droplets, 1 was positive for KIT D816V and 28693 were positive for WT. Of all KIT-positive droplets, 7,69% was single-positive.

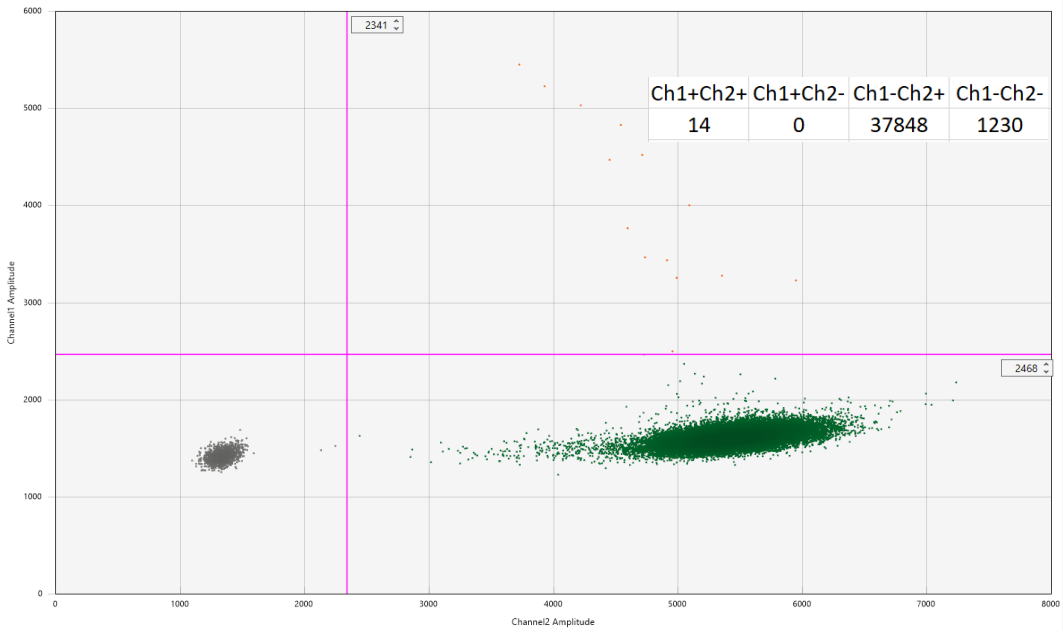

Figure 20: 2D graph of patient P18, with channel 1 amplitude (mutant) on the y-axis and channel 2 amplitude (WT) on the x-axis. Y-axis (2341) and X-axis (2468) thresholds are shown next to the corresponding line. Single KIT-positive droplets are marked by blue droplets. The orange droplets show droplets positive for both channels. Green droplets represent droplets that are solely positive for WT, and grey droplets depict double negative droplets. The number of droplets within each group is shown as well.

In figure 20, the 2D spectrum of patient P18 is shown. With 2 wells combined, 14 droplets were found to be double-positive. Out of the single-positive droplets, 0 were positive for KIT D816V and 37848 for WT.

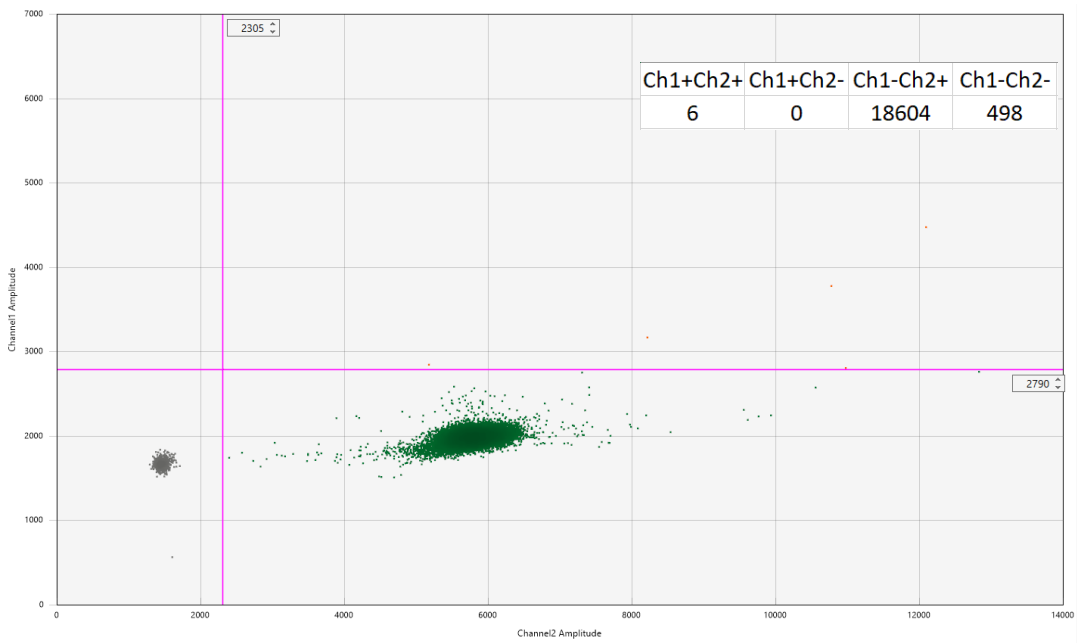

Figure 21: 2D graph of patient P19, with channel 1 amplitude (mutant) on the y-axis and channel 2 amplitude (WT) on the x-axis. Y-axis (2305) and X-axis (2790) thresholds are shown next to the corresponding line. Single KIT-positive droplets are marked by blue droplets. The orange droplets show droplets positive for both channels. Green droplets represent droplets that are solely positive for WT, and grey droplets depict double negative droplets. The number of droplets within each group is shown as well.

In figure 21, the 2D spectrum of patient P19 is shown. With 2 wells combined, 6 droplets were found to be double-positive. Out of the single-positive droplets, 0 were positive for KIT D816V and 18604 for WT.

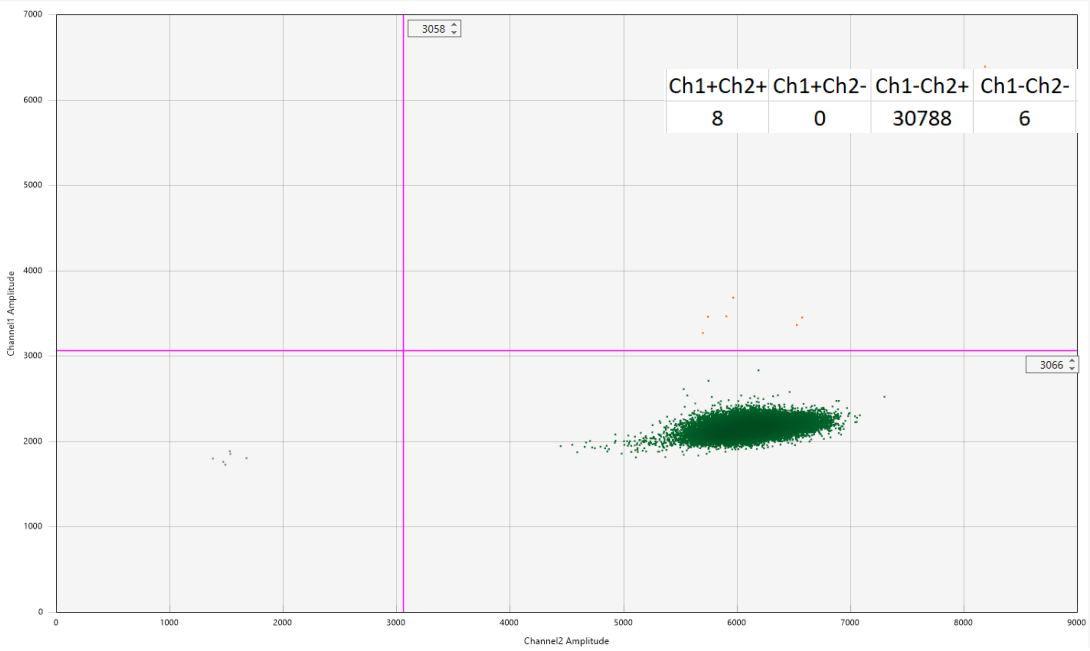

Figure 22: 2D graph of patient P20, with channel 1 amplitude (mutant) on the y-axis and channel 2 amplitude (WT) on the x-axis. Y-axis (3058) and X-axis (3066) thresholds are shown next to the corresponding line. Single KIT-positive droplets are marked by blue droplets. The orange droplets show droplets positive for both channels. Green droplets represent droplets that are solely positive for WT, and grey droplets depict double negative droplets. The number of droplets within each group is shown as well.

In figure 22, the 2D spectrum of patient P20 is shown. With 2 wells combined, 8 droplets were found to be double-positive. Out of the single-positive droplets, 0 were positive for KIT D816V and 30788 for WT.

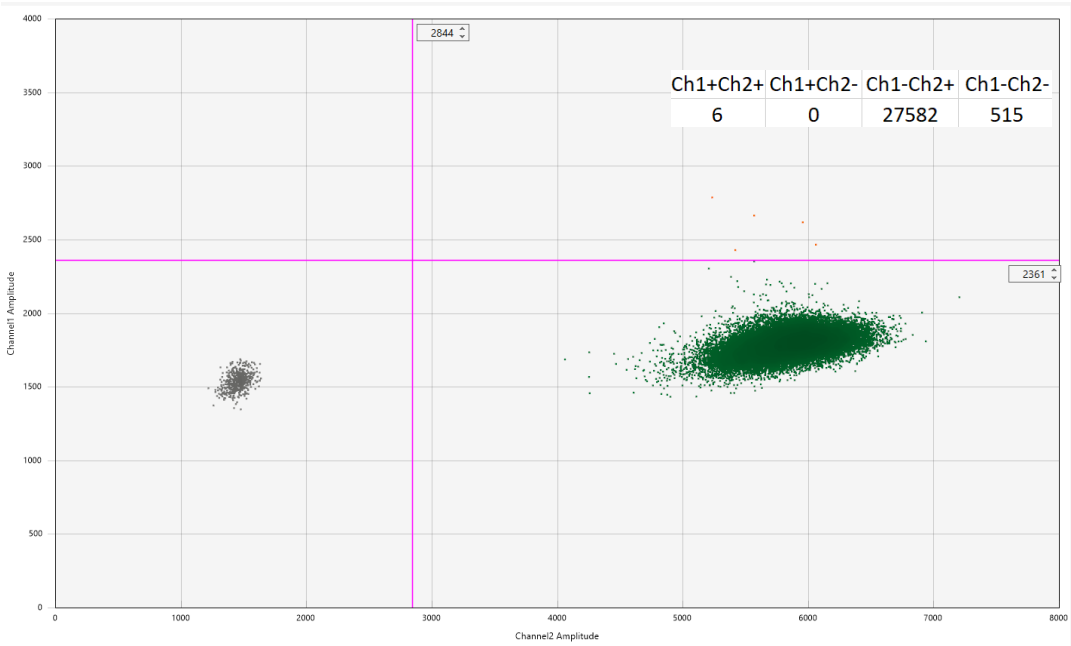

Figure 23: 2D graph of patient P21, with channel 1 amplitude (mutant) on the y-axis and channel 2 amplitude (WT) on the x-axis. Y-axis (2844) and X-axis (2361) thresholds are shown next to the corresponding line. Single KIT-positive droplets are marked by blue droplets. The orange droplets show droplets positive for both channels. Green droplets represent droplets that are solely positive for WT, and grey droplets depict double negative droplets. The number of droplets within each group is shown as well.

In figure 23, the 2D spectrum of patient P21 is shown. With 2 wells combined, 6 droplets were found to be double-positive. Out of the single-positive droplets, 0 were positive for KIT D816V and 27582 for WT.

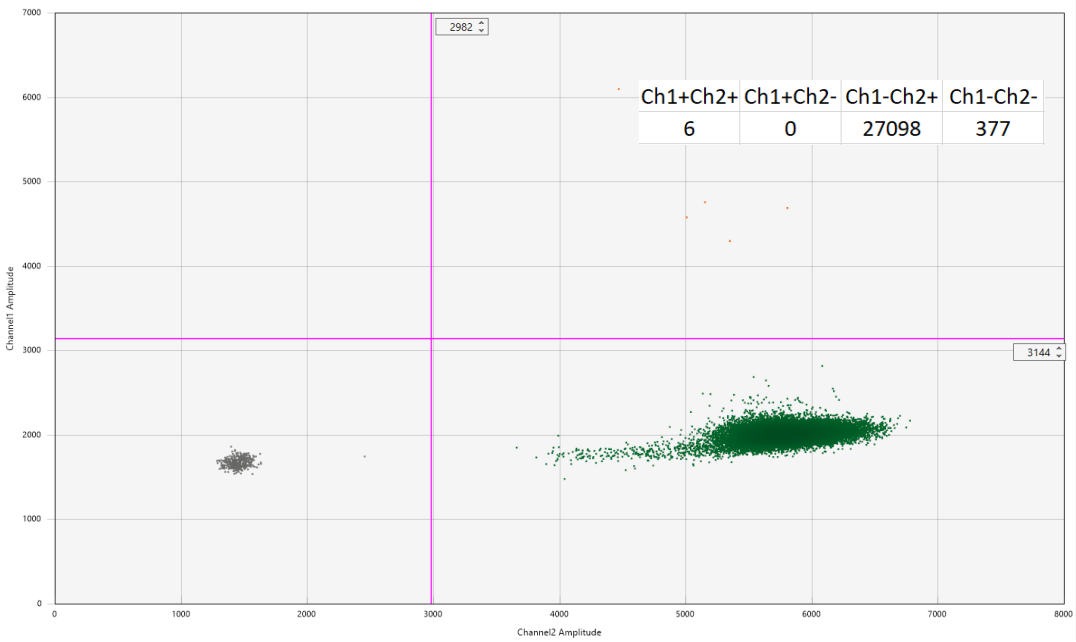

Figure 24: 2D graph of patient P22, with channel 1 amplitude (mutant) on the y-axis and channel 2 amplitude (WT) on the x-axis. Y-axis (2982) and X-axis (3144) thresholds are shown next to the corresponding line. Single KIT-positive droplets are marked by blue droplets. The orange droplets show droplets positive for both channels. Green droplets represent droplets that are solely positive for WT, and grey droplets depict double negative droplets. The number of droplets within each group is shown as well.

In figure 24, the 2D spectrum of patient P22 is shown. With 2 wells combined, 6 droplets were found to be double-positive. Out of the single-positive droplets, 0 were positive for KIT D816V and 27098 for WT.

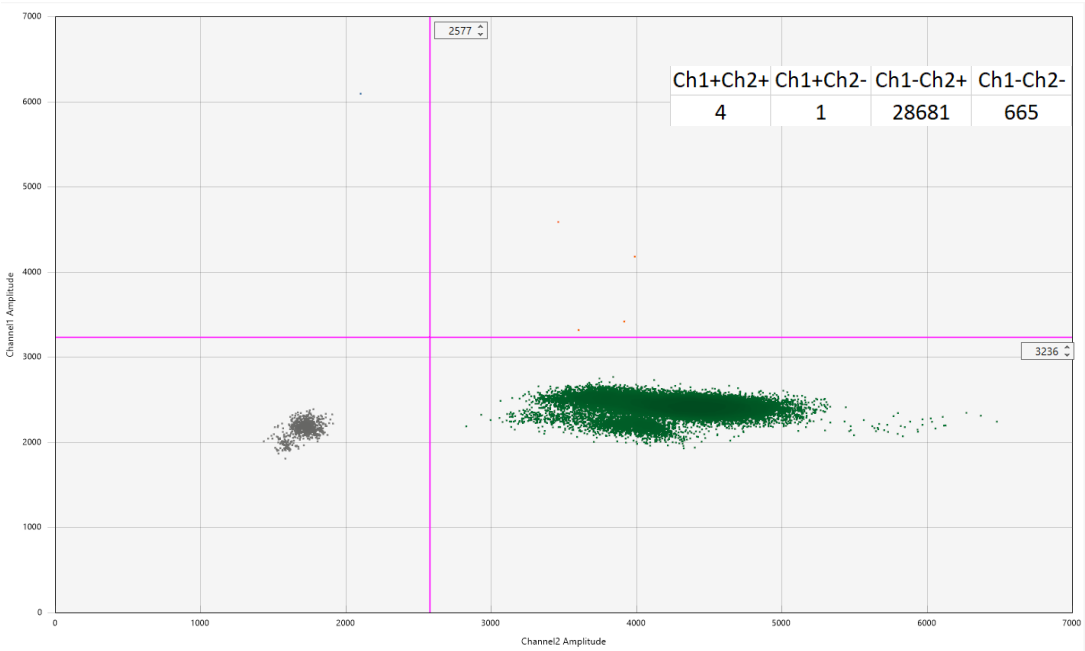

Figure 25: 2D graph of patient P23, with channel 1 amplitude (mutant) on the y-axis and channel 2 amplitude (WT) on the x-axis. Y-axis (2577) and X-axis (3236) thresholds are shown next to the corresponding line. Single KIT-positive droplets are marked by blue droplets. The orange droplets show droplets positive for both channels. Green droplets represent droplets that are solely positive for WT, and grey droplets depict double negative droplets. The number of droplets within each group is shown as well.

In figure 25, the 2D spectrum of patient P23 is shown. With 2 wells combined, 4 droplets were found to be double-positive. Out of the single-positive droplets, 1 was positive for KIT D816V and 28681 were positive for WT. Of all KIT-positive droplets, 20,0% was single-positive.

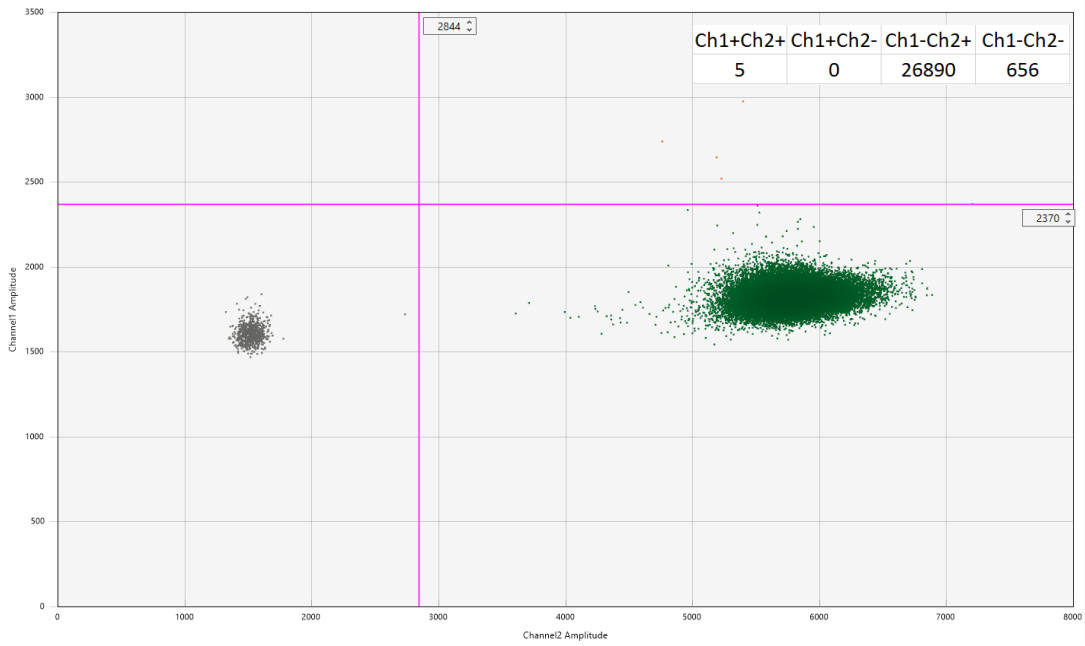

Figure 26: 2D graph of patient P24, with channel 1 amplitude (mutant) on the y-axis and channel 2 amplitude (WT) on the x-axis. Y-axis (2844) and X-axis (2370) thresholds are shown next to the corresponding line. Single KIT-positive droplets are marked by blue droplets. The orange droplets show droplets positive for both channels. Green droplets represent droplets that are solely positive for WT, and grey droplets depict double negative droplets. The number of droplets within each group is shown as well.

In figure 26, the 2D spectrum of patient P24 is shown. With 2 wells combined, 5 droplets were found to be double-positive. Out of the single-positive droplets, 0 were positive for KIT D816V and 26890 for WT.

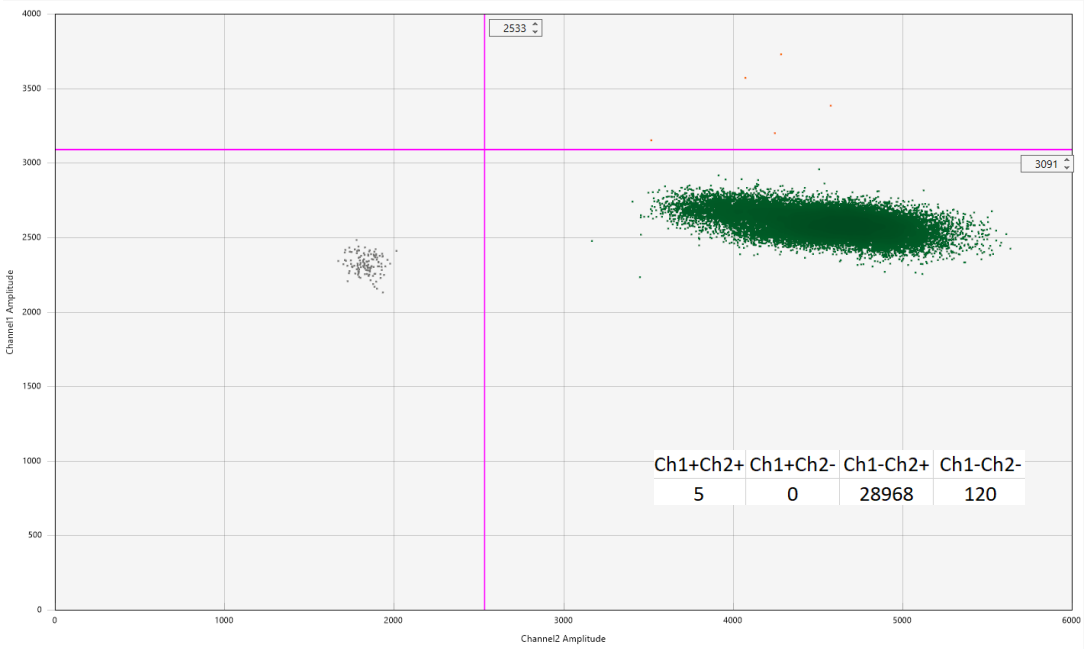

Figure 27: 2D graph of patient P25, with channel 1 amplitude (mutant) on the y-axis and channel 2 amplitude (WT) on the x-axis. Y-axis (2533) and X-axis (3091) thresholds are shown next to the corresponding line. Single KIT-positive droplets are marked by blue droplets. The orange droplets show droplets positive for both channels. Green droplets represent droplets that are solely positive for WT, and grey droplets depict double negative droplets. The number of droplets within each group is shown as well.

In figure 27, the 2D spectrum of patient P25 is shown. With 2 wells combined, 5 droplets were found to be double-positive. Out of the single-positive droplets, 0 were positive for KIT D816V and 28968 for WT.

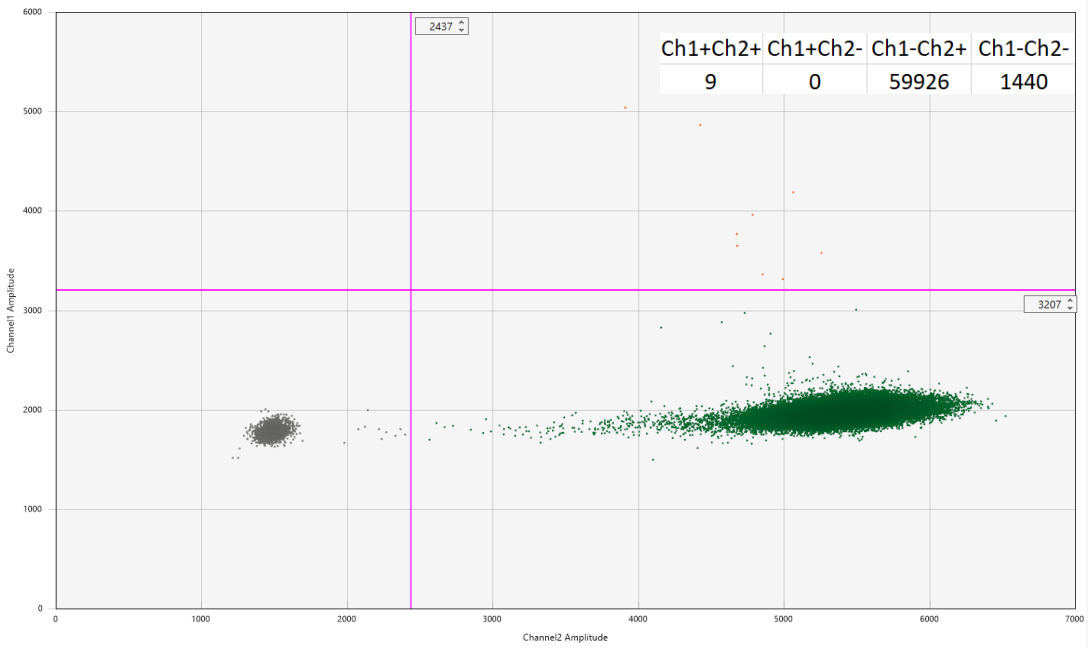

Figure 28: 2D graph of patient P26, with channel 1 amplitude (mutant) on the y-axis and channel 2 amplitude (WT) on the x-axis. Y-axis (2437) and X-axis (3207) thresholds are shown next to the corresponding line. Single KIT-positive droplets are marked by blue droplets. The orange droplets show droplets positive for both channels. Green droplets represent droplets that are solely positive for WT, and grey droplets depict double negative droplets. The number of droplets within each group is shown as well.

In figure 28, the 2D spectrum of patient P26 is shown. With 4 wells combined, 9 droplets were found to be double-positive. Out of the single-positive droplets, 0 were positive for KIT D816V and 59926 for WT.

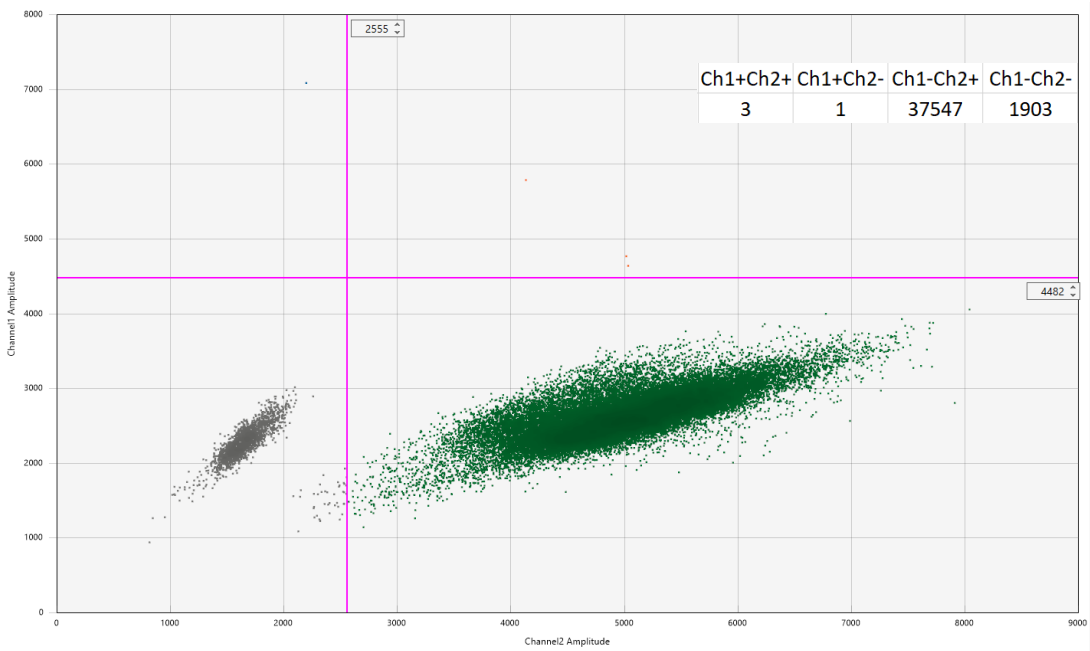

Figure 29: 2D graph of patient P27, with channel 1 amplitude (mutant) on the y-axis and channel 2 amplitude (WT) on the x-axis. Y-axis (2555) and X-axis (4482) thresholds are shown next to the corresponding line. Single KIT-positive droplets are marked by blue droplets. The orange droplets show droplets positive for both channels. Green droplets represent droplets that are solely positive for WT, and grey droplets depict double negative droplets. The number of droplets within each group is shown as well.

In figure 29, the 2D spectrum of patient P27 is shown. With 2 wells combined, 3 droplets were found to be double-positive. Out of the single-positive droplets, 1 was positive for KIT D816V and 37547 were positive for WT. Of all KIT-positive droplets, 25,0% was single-positive.

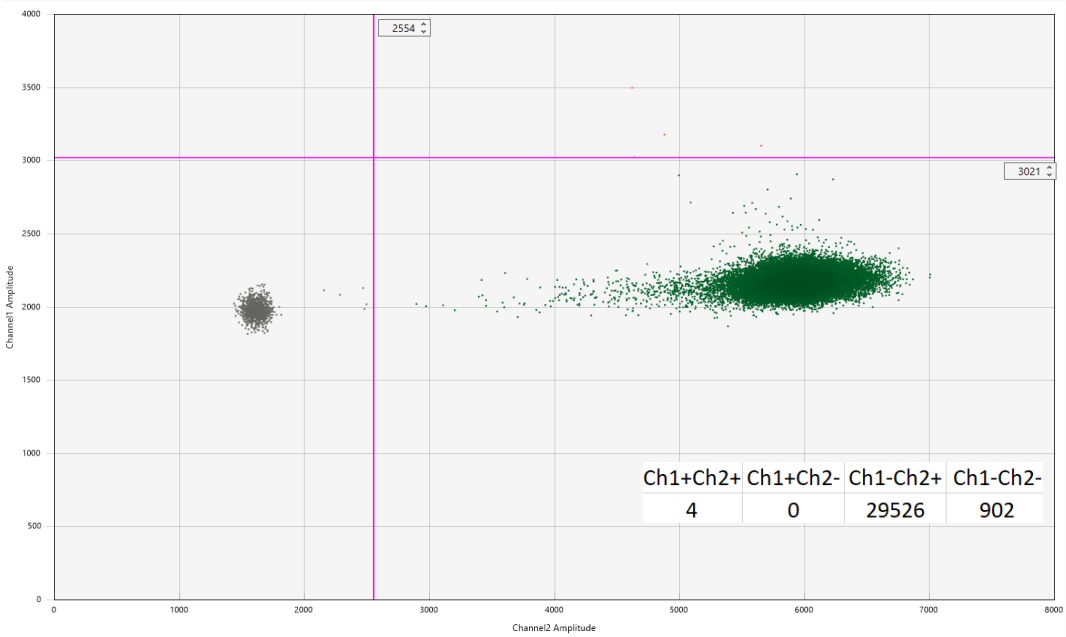

Figure 30: 2D graph of patient P28, with channel 1 amplitude (mutant) on the y-axis and channel 2 amplitude (WT) on the x-axis. Y-axis (2554) and X-axis (3021) thresholds are shown next to the corresponding line. Single KIT-positive droplets are marked by blue droplets. The orange droplets show droplets positive for both channels. Green droplets represent droplets that are solely positive for WT, and grey droplets depict double negative droplets. The number of droplets within each group is shown as well.

In figure 30, the 2D spectrum of patient P28 is shown. With 2 wells combined, 4 droplets were found to be double-positive. Out of the single-positive droplets, 0 were positive for KIT D816V and 29526 for WT.

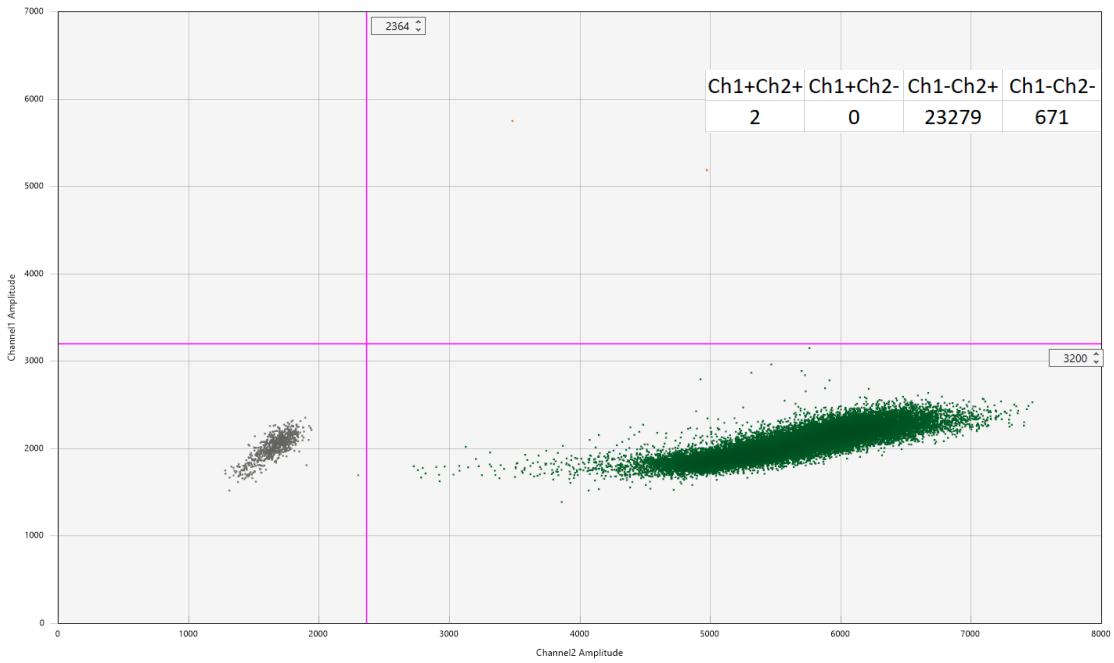

Figure 31: 2D graph of patient P29, with channel 1 amplitude (mutant) on the y-axis and channel 2 amplitude (WT) on the x-axis. Y-axis (2364) and X-axis (3200) thresholds are shown next to the corresponding line. Single KIT-positive droplets are marked by blue droplets. The orange droplets show droplets positive for both channels. Green droplets represent droplets that are solely positive for WT, and grey droplets depict double negative droplets. The number of droplets within each group is shown as well.

In figure 31, the 2D spectrum of patient P29 is shown. With 2 wells combined, 2 droplets were found to be double-positive. Out of the single-positive droplets, 0 were positive for KIT D816V and 23279 for WT.

Appendix 5: Overview of NGS data

Appendix 5 is included within the supplementary data: *Appendix 5. NGS data overview.xlsx*